Magnetic Reconnection in Accretion Disks and Coronae

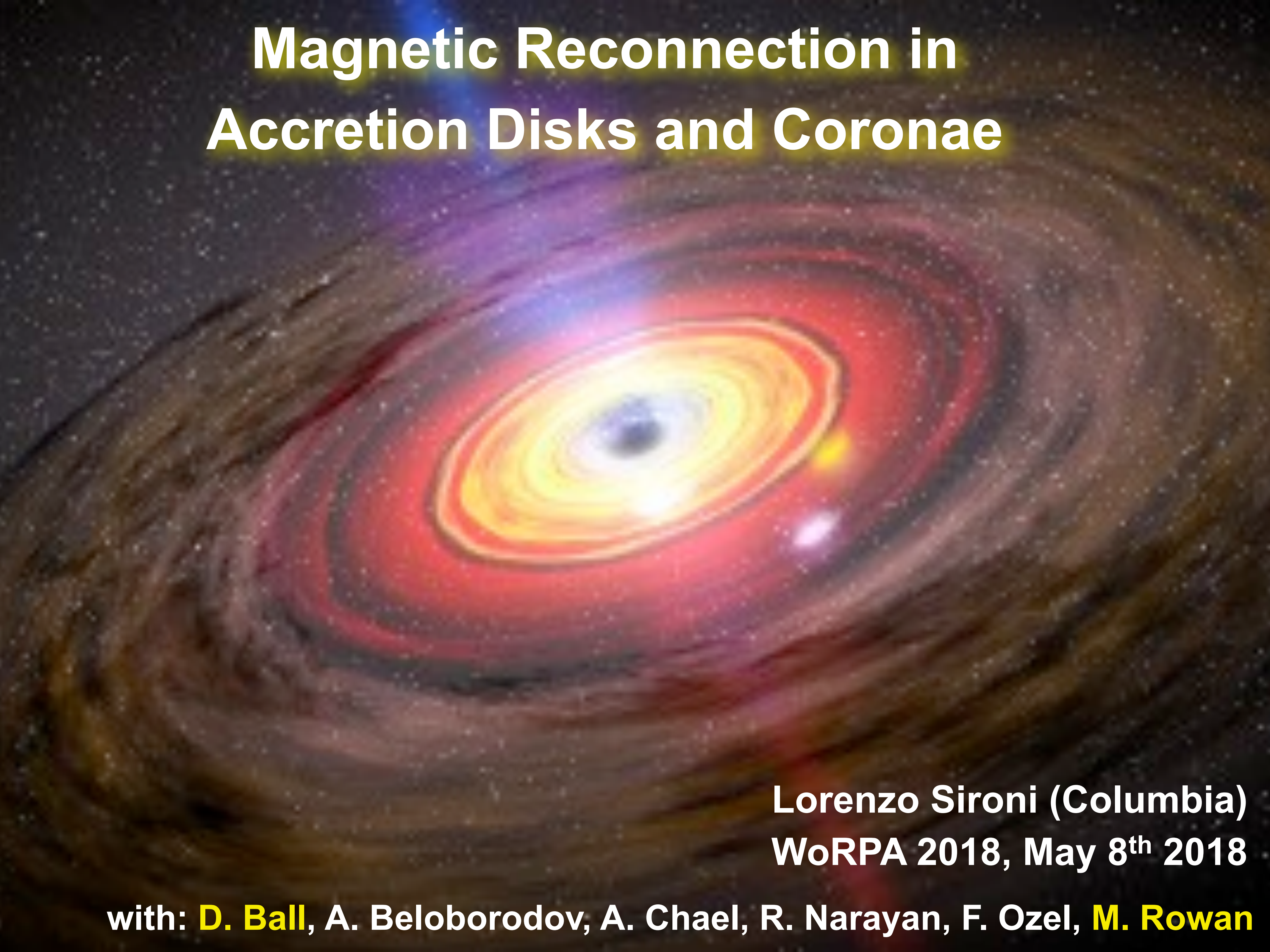

Lorenzo Sironi (Columbia)

WoRPA 2018, May 8th 2018

with: D. Ball, A. Beloborodov, A. Chael, R. Narayan, F. Ozel, M. Rowan

Outline

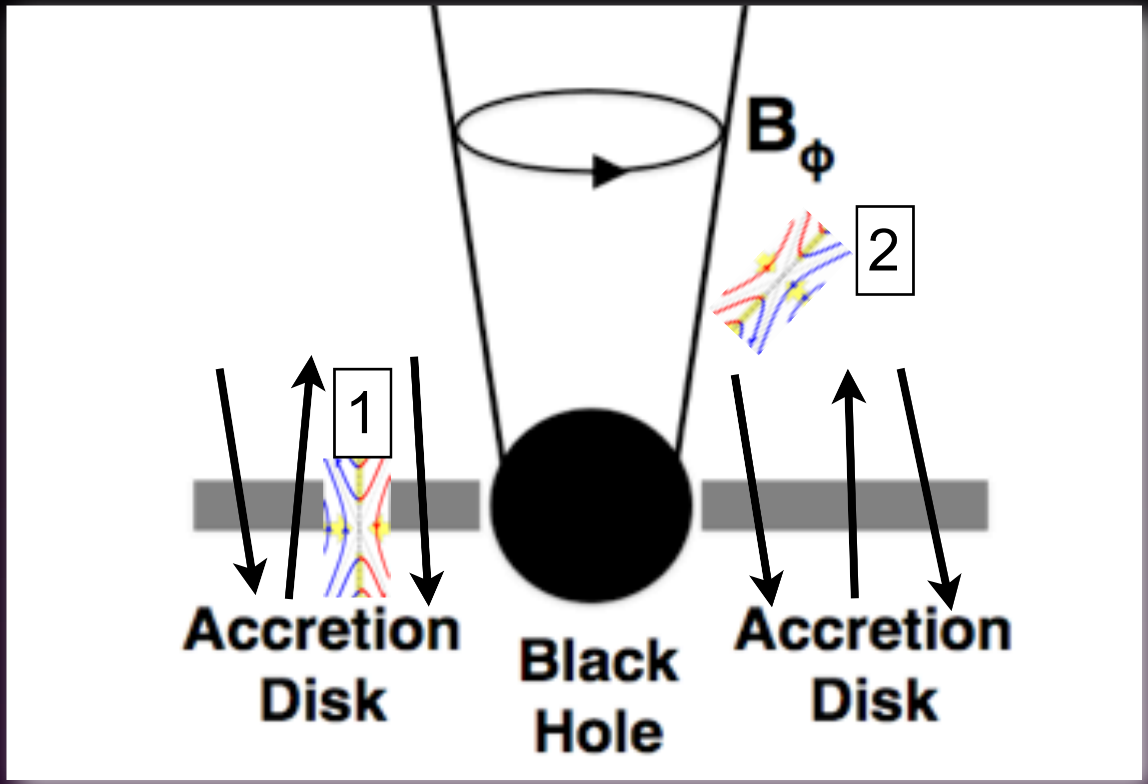

(1). Magnetized disks and coronae of collisionless accretion flows (like Sgr A* in our Galactic Center).

- Trans-relativistic reconnection (σ~1), electron-proton plasma.

(2). Magnetized coronae in bright accreting binaries (Cyg X-1).

- Trans- and ultra-relativistic reconnection (σ~10) in strong radiation fields, pair-dominated.

Where reconnection?

Global current sheets

from accreting field loops

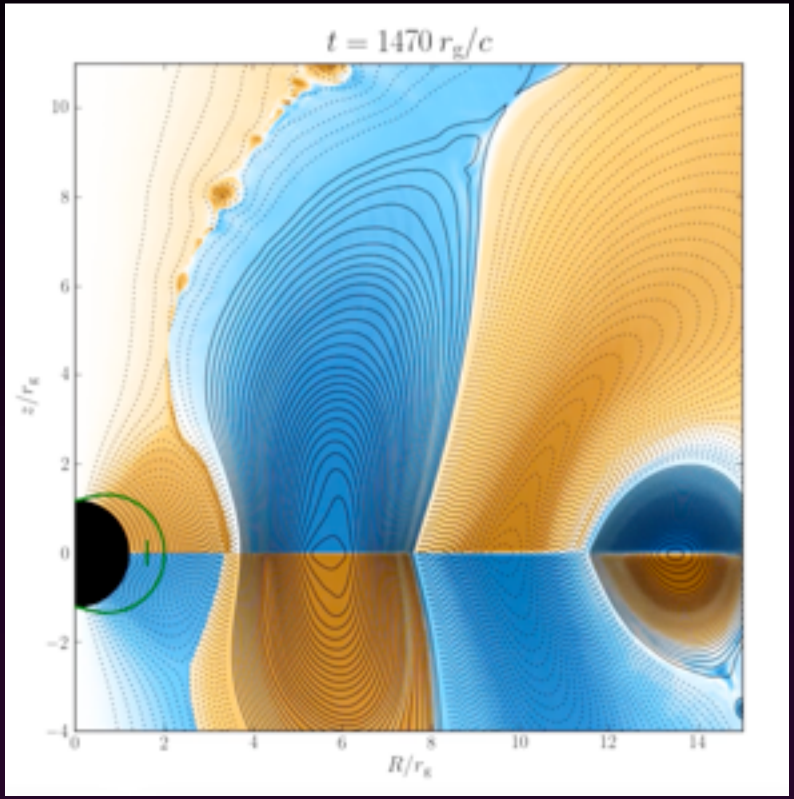

(Parfrey, Giannios & Beloborodov 2015)

Where reconnection?

Global current sheets

from accreting field loops

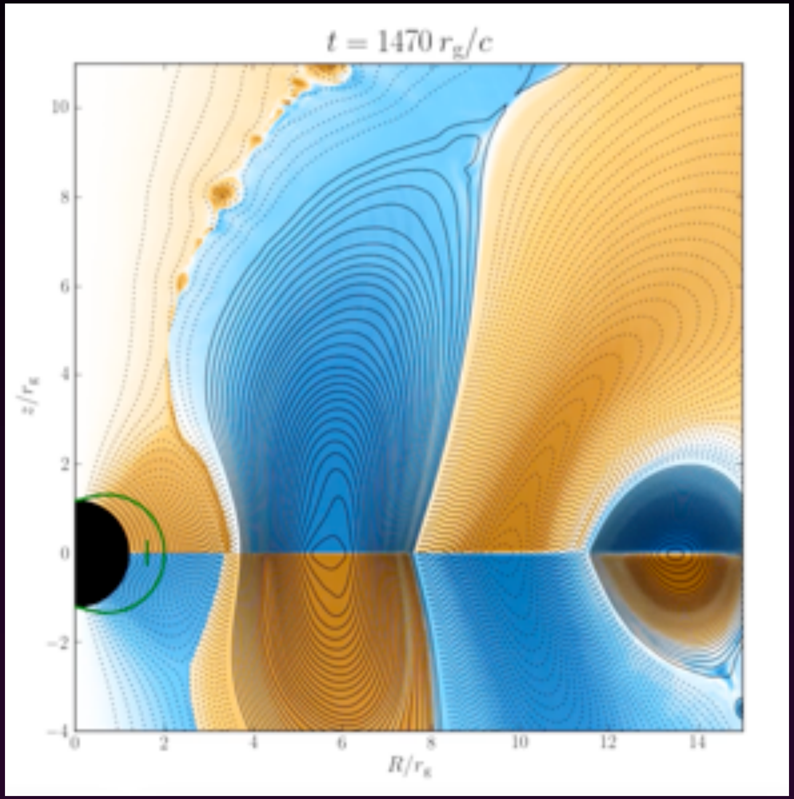

(Parfrey, Giannios & Beloborodov 2015)

Local current sheets

MRI → turbulence → reconnection

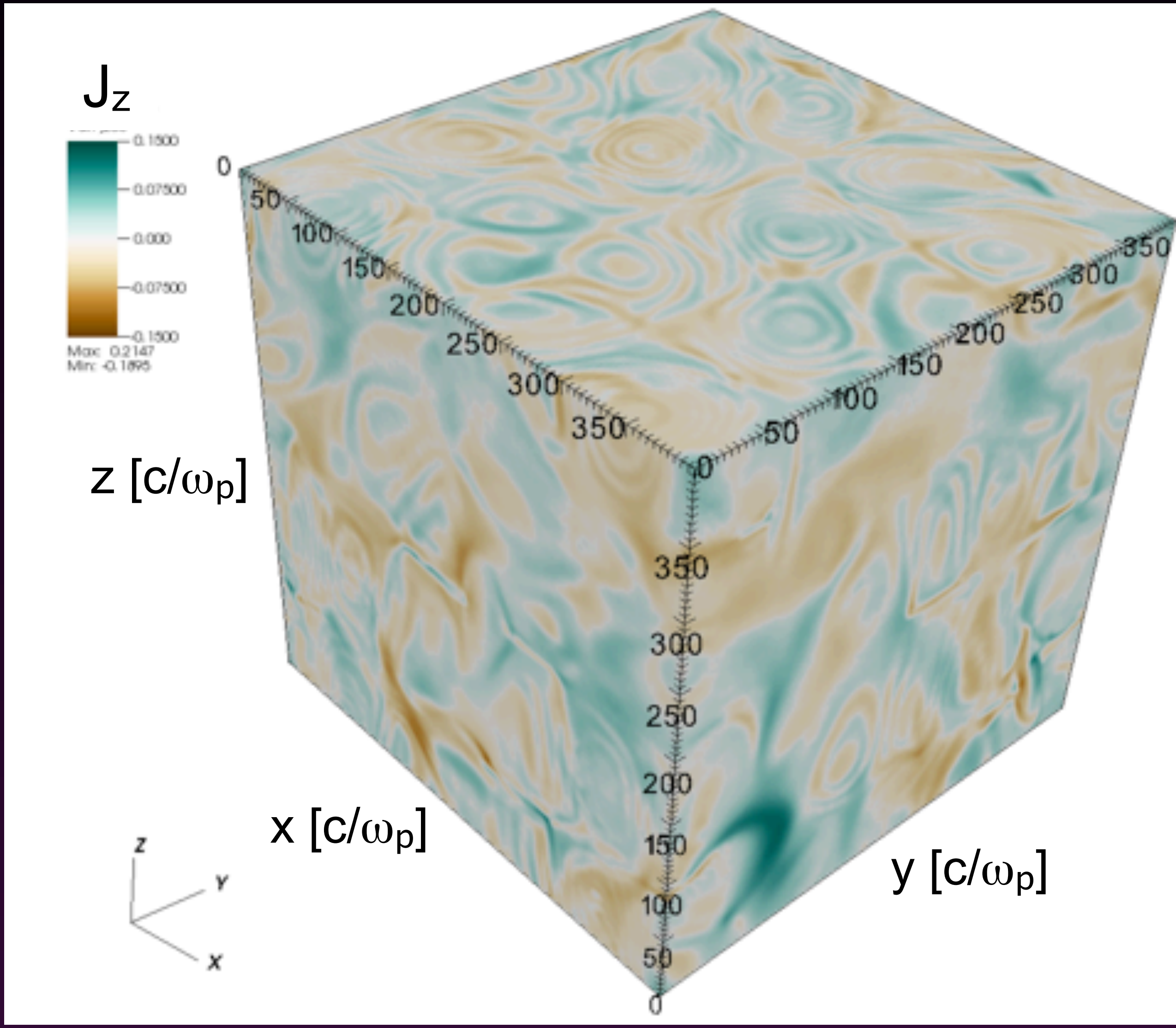

[see Luca Comisso's talk]

1. Trans-relativistic reconnection in low-luminosity accretion flows

Sgr A*, our neighbor

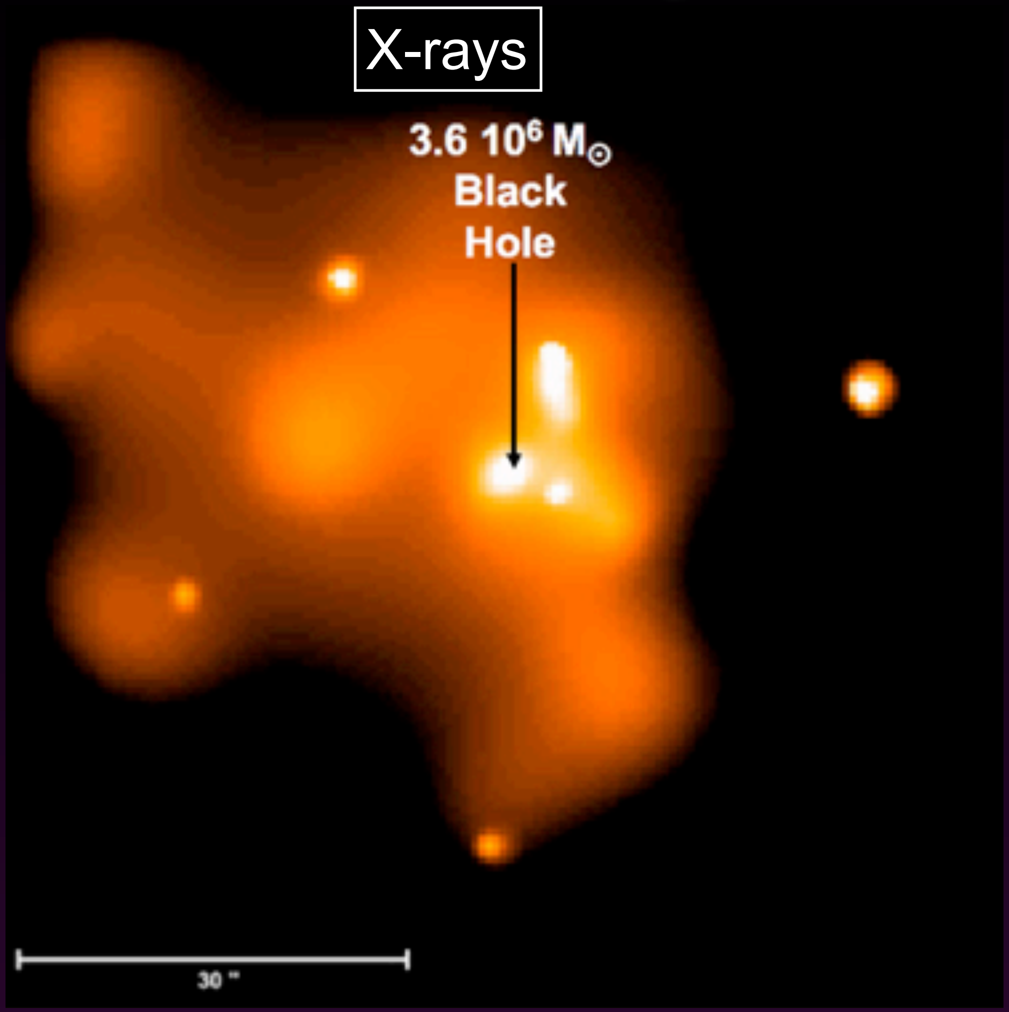

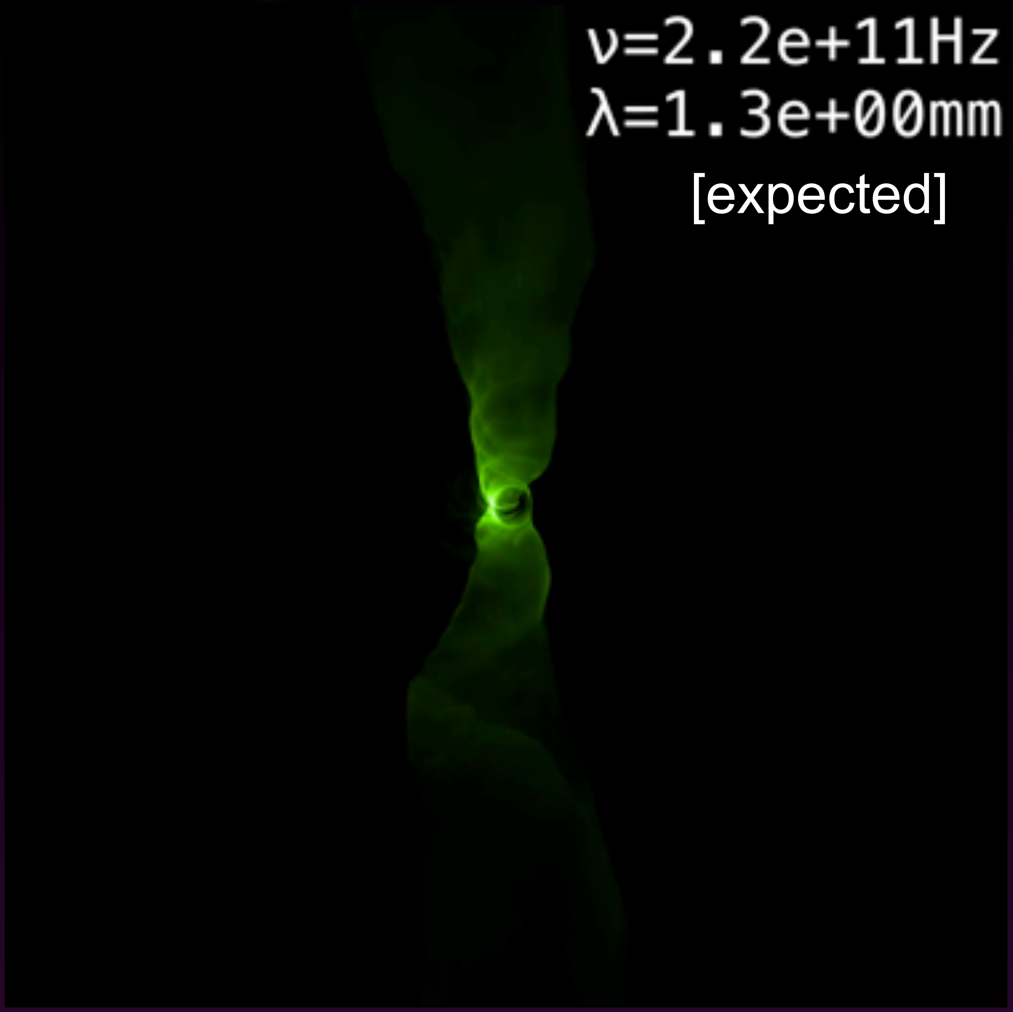

- The Chandra X-ray telescope allows to probe the properties of the gas around the BH, on scales of order $\sim 10^5$ gravitational radii.
- The Event Horizon Telescope (EHT) is going to probe the gas in the immediate vicinity of the BH.

Thermal and non-thermal electrons

Sgr A* : spectrum

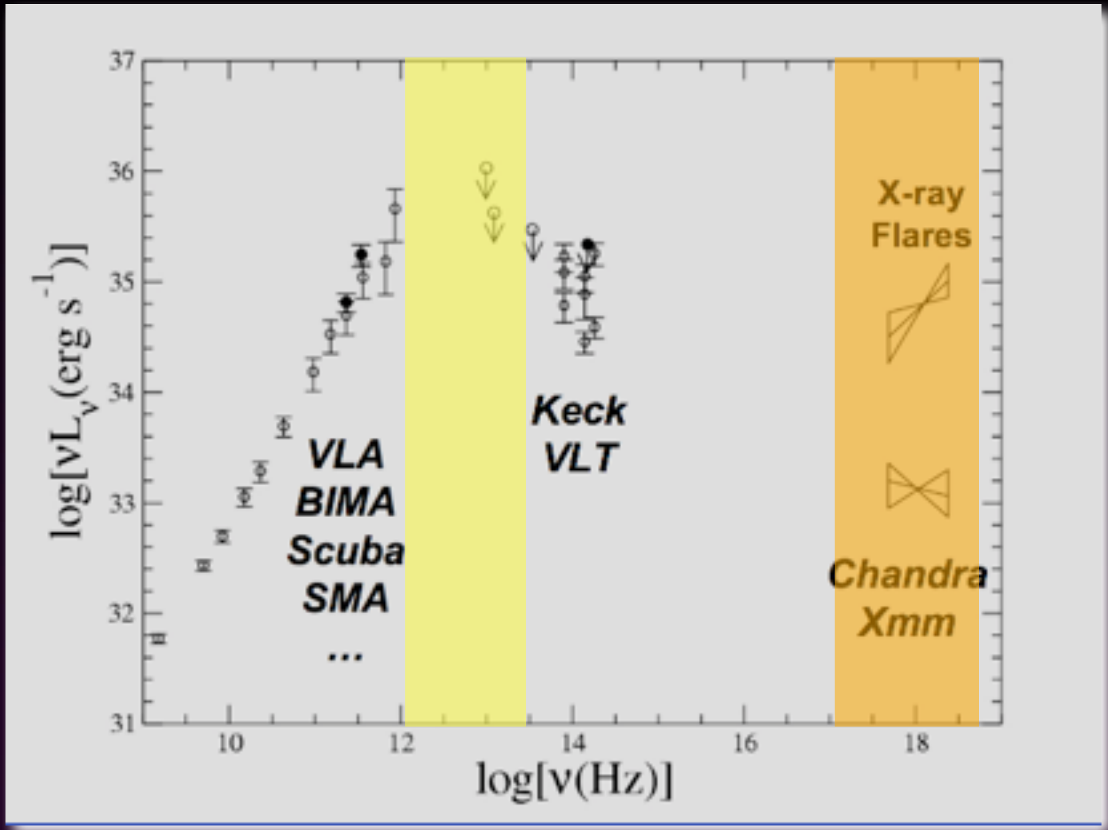

- Thermal trans-relativistic electrons (with T_e/T_p~0.3) are invoked to explain the peak of Sgr A* spectrum.

- Non-thermal electrons are invoked to explain the spectrum and time variability of X-ray flares from Sgr A* (Ponti+ 17).

Reconnection sites in Sgr A*

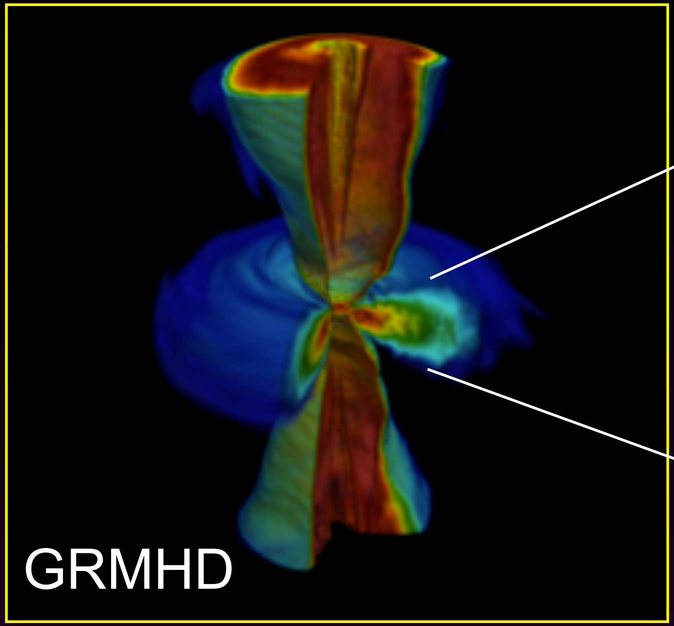

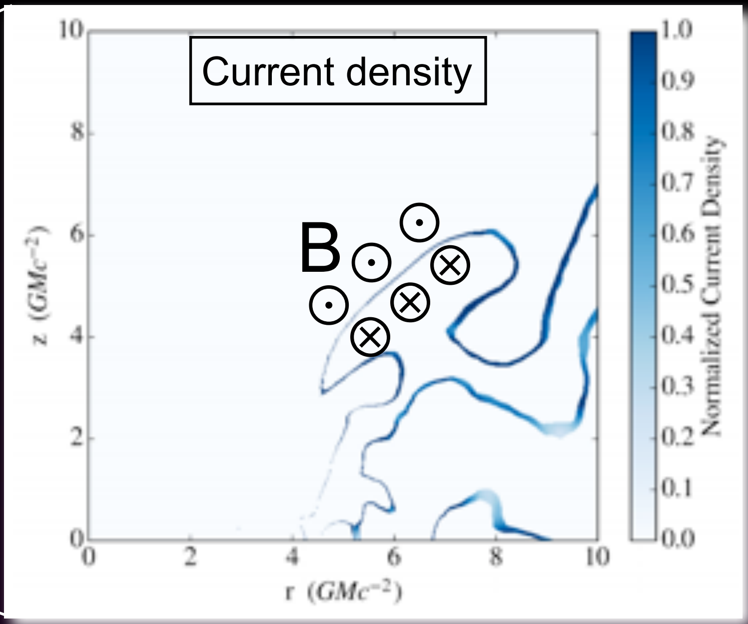

Reconnection current sheets

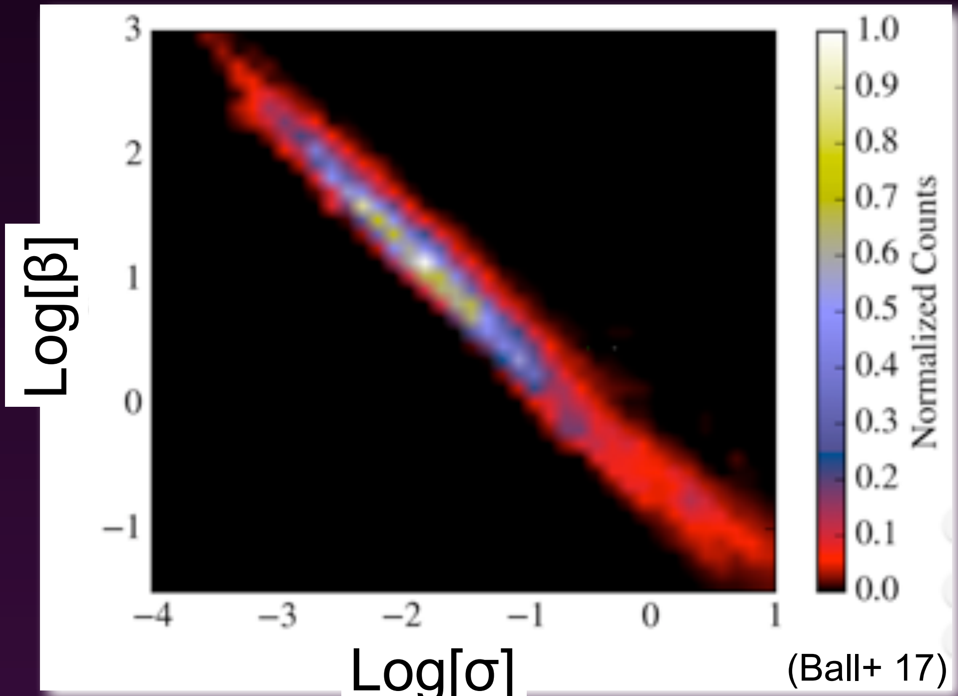

(Ball+ 17)

- The plasma around reconnection layers spans a range of beta and sigma.

$$\beta = \frac{8\pi n_0 k_B T}{B_0^2} \qquad \sigma = \frac{B_0^2}{4\pi w}$$

Flow dynamics and particle heating

Dependence on beta

σ=0.1 β=0.01, realistic mass ratio

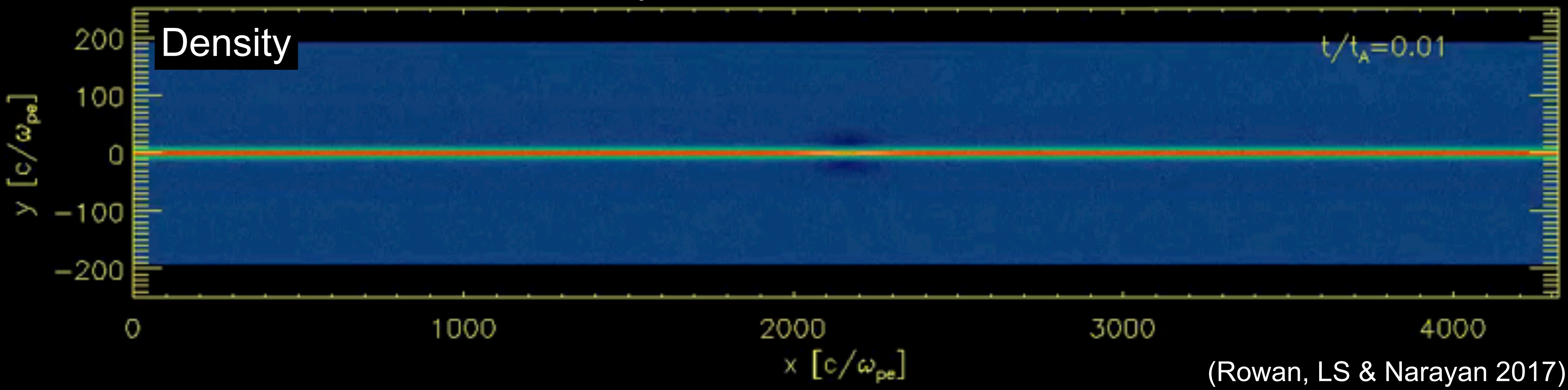

(Rowan, LS & Narayan 2017)

- Low beta: the outflow is fragmented into a number of secondary plasmoids.

Dependence on beta

σ=0.1 β=0.01, realistic mass ratio

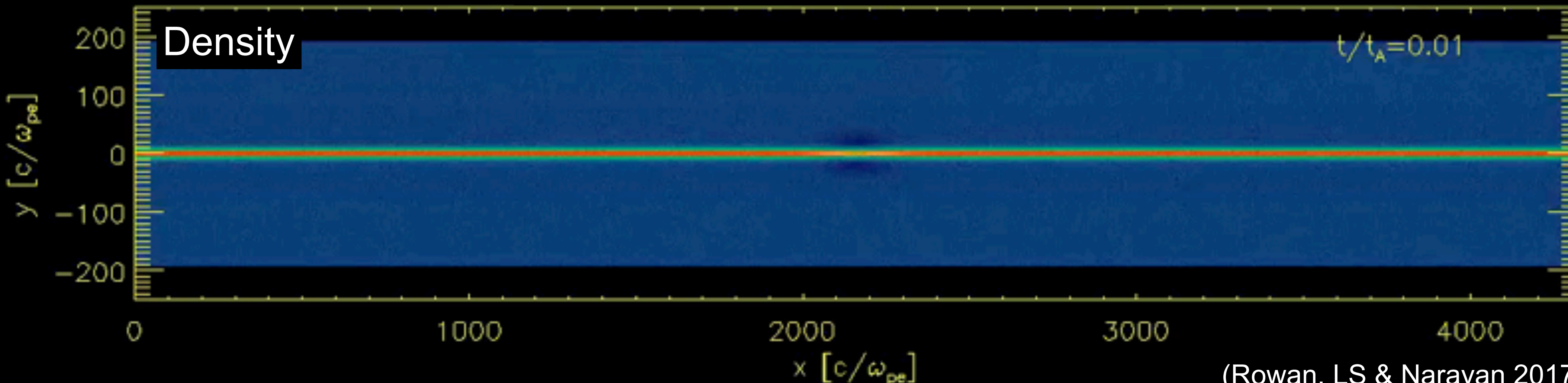

(Rowan, LS & Narayan 2017)

- Low beta: the outflow is fragmented into a number of secondary plasmoids.

σ=0.1 β=2, realistic mass ratio

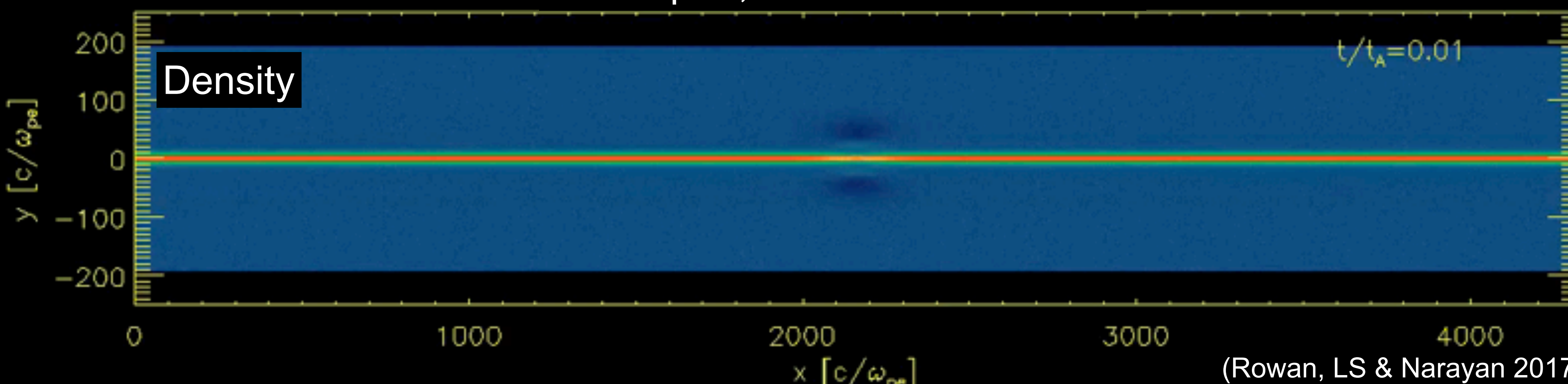

(Rowan, LS & Narayan 2017)

- High beta: smooth outflow, no secondary plasmoids.

Inflows and outflows

Inflow

Outflow

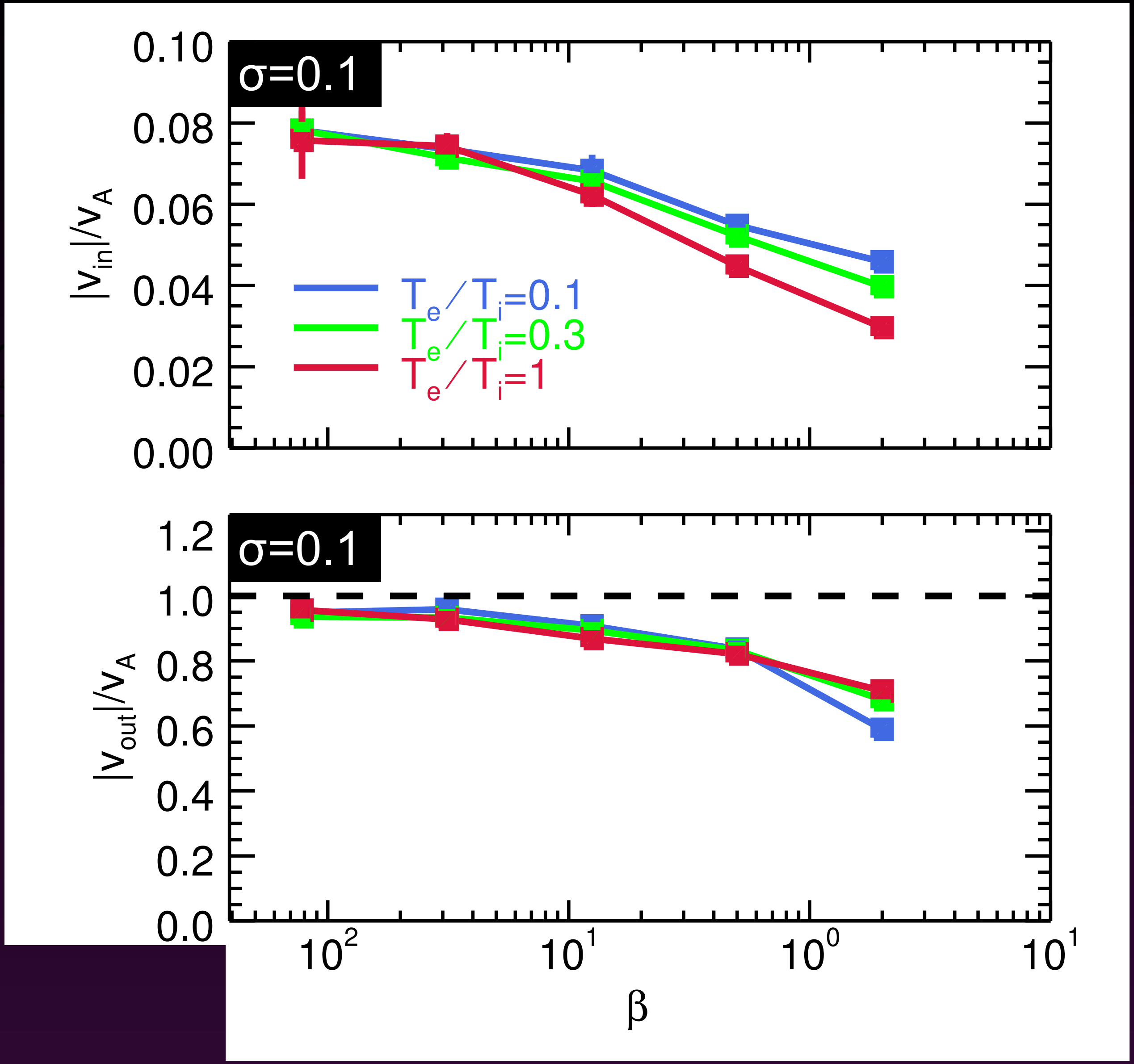

Alfven speed

$$v_A = c\sqrt{\frac{\sigma}{1+\sigma}}$$

(Rowan, LS & Narayan 2017)

- Both the inflow speed and the outflow speed decrease at high beta (relative to the Alfven speed), regardless of the temperature ratio.

Characterization of heating

- Blue: upstream region, starting above the current sheet.
- Red: upstream region, starting below the current sheet.
- White/yellow: mix of blue and red particles → downstream region.

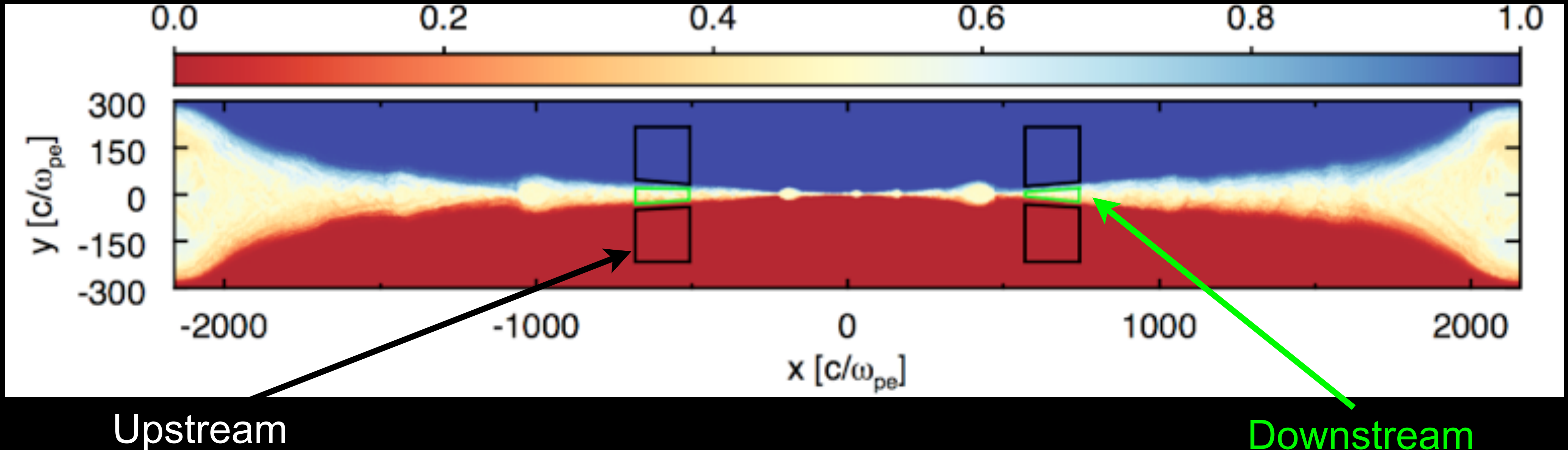

Define total electron heating as

$$M_{ue,\mathrm{tot}} \equiv \frac{\upsilon_{\mathrm{e,down}} - \upsilon_{\mathrm{e,up}}}{\sigma\, m_{\mathrm{i}}/m_{\mathrm{e}}}$$

υ=internal energy per unit rest mass.

alternatively,

$$M_{Te,\mathrm{tot}} \equiv \frac{\theta_{\mathrm{e,down}} - \theta_{\mathrm{e,up}}}{\sigma\, m_{\mathrm{i}}/m_{\mathrm{e}}}$$

θ=dimensionless temperature.

(Shay et al. 2014)

and then separate adiabatic and irreversible contributions.

Electron heating efficiency

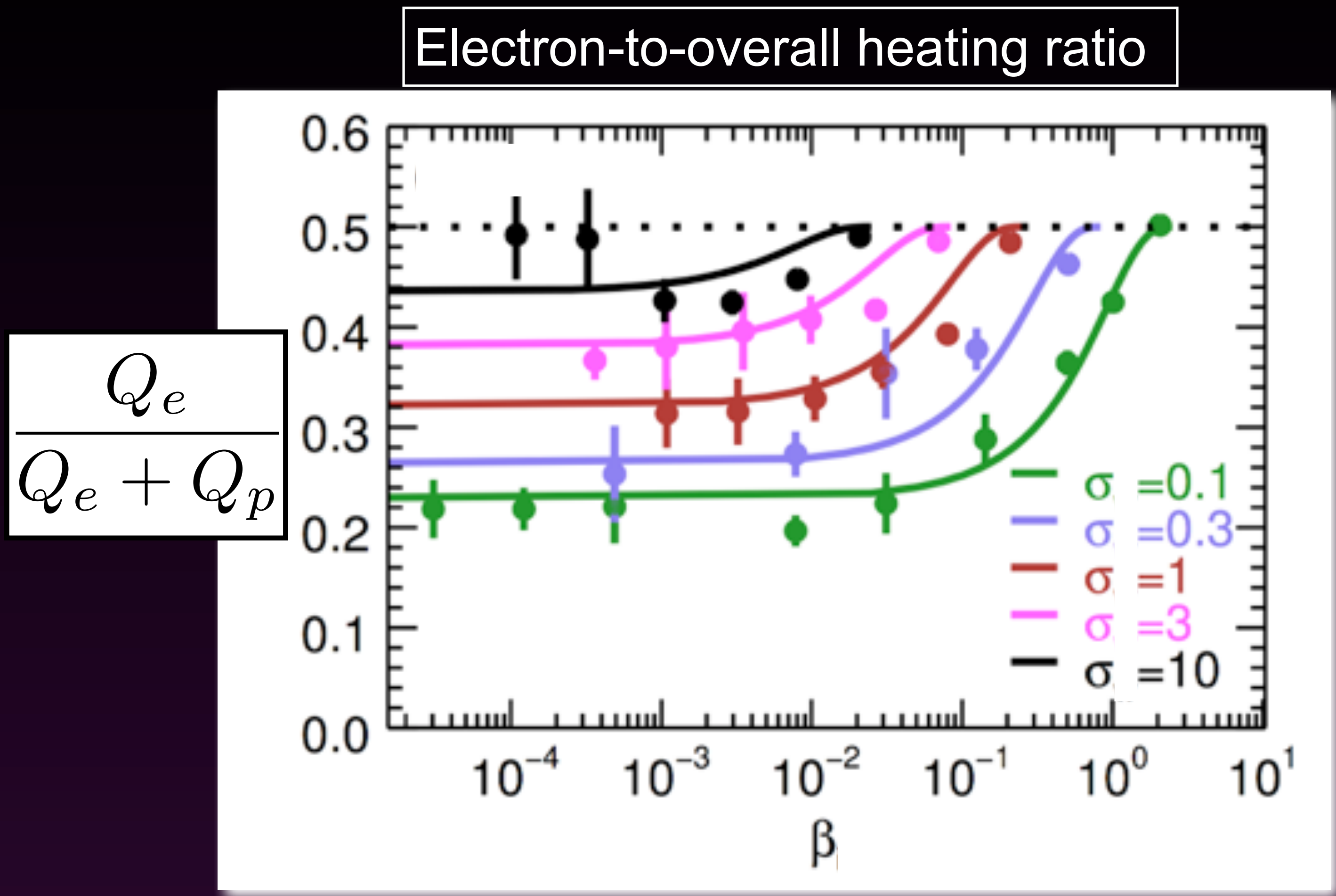

The curves extend up to β_{max}~1/(4σ)

(Rowan, LS & Narayan 2017)

- Electrons are always heated less then protons (for σ≪1, the ratio is ~0.2).
- Comparable heating efficiencies:
  - at high beta, when both species already start relativistically hot.
  - in ultra-relativistic (σ≫1) reconnection.

Electron heating as a subgrid model

GRMHD simulation by A. Chael

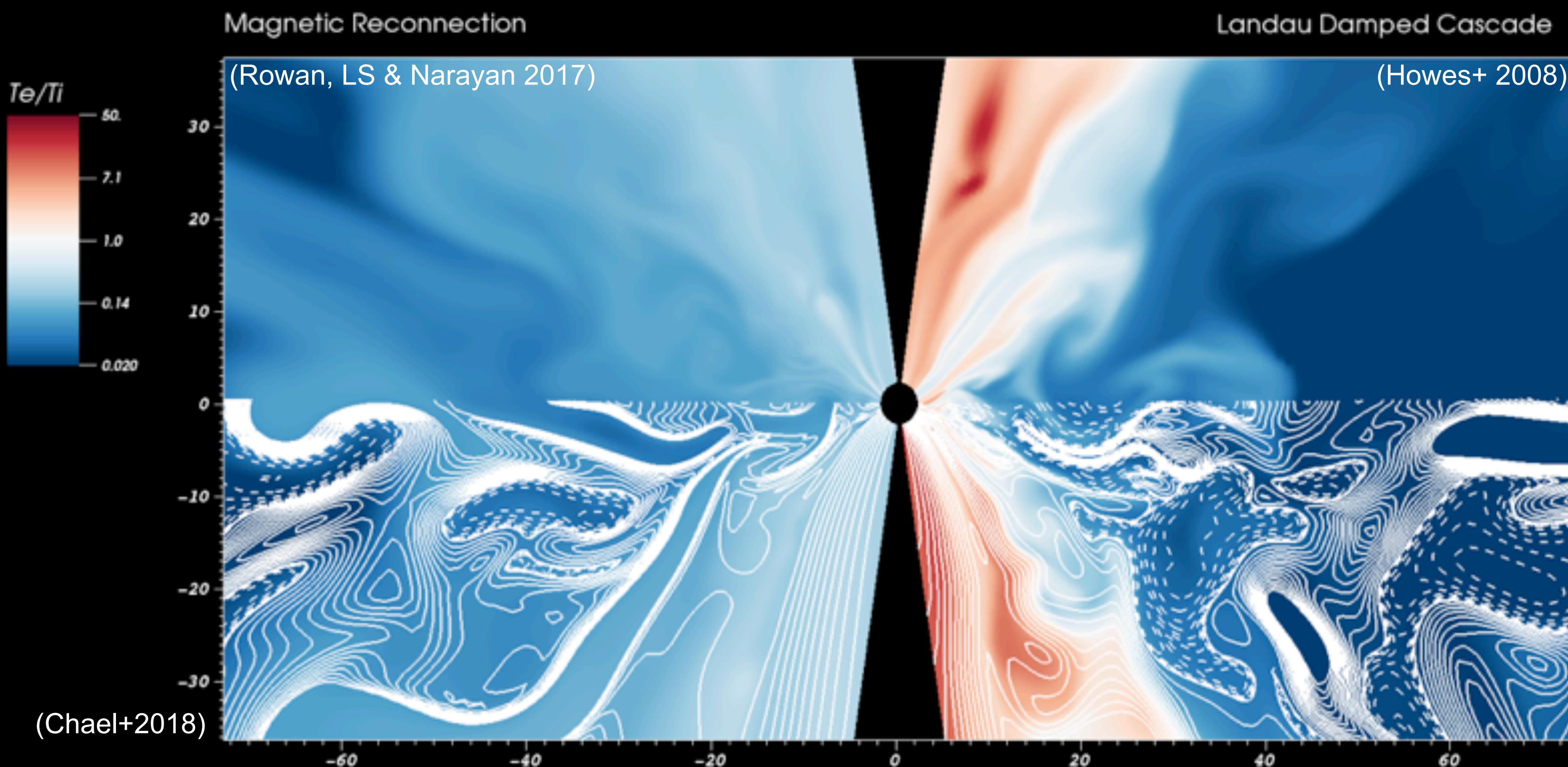

(Chael+2018)

- Electrons always colder than protons.
- Disk electrons are hotter than in Howes' prescription.

- Electrons hotter than protons in the jet.
- Disk electrons are colder than in Rowan's prescription.

Particle acceleration

Electron and proton acceleration

σ=0.3 β=0.0003, realistic mass ratio

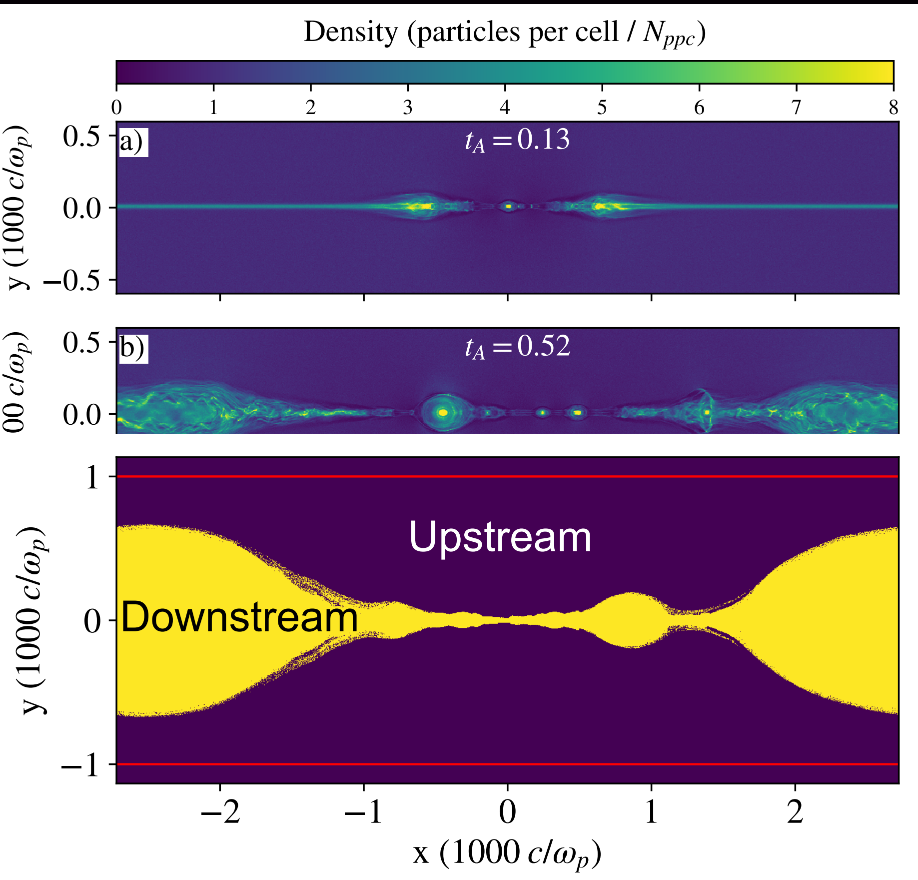

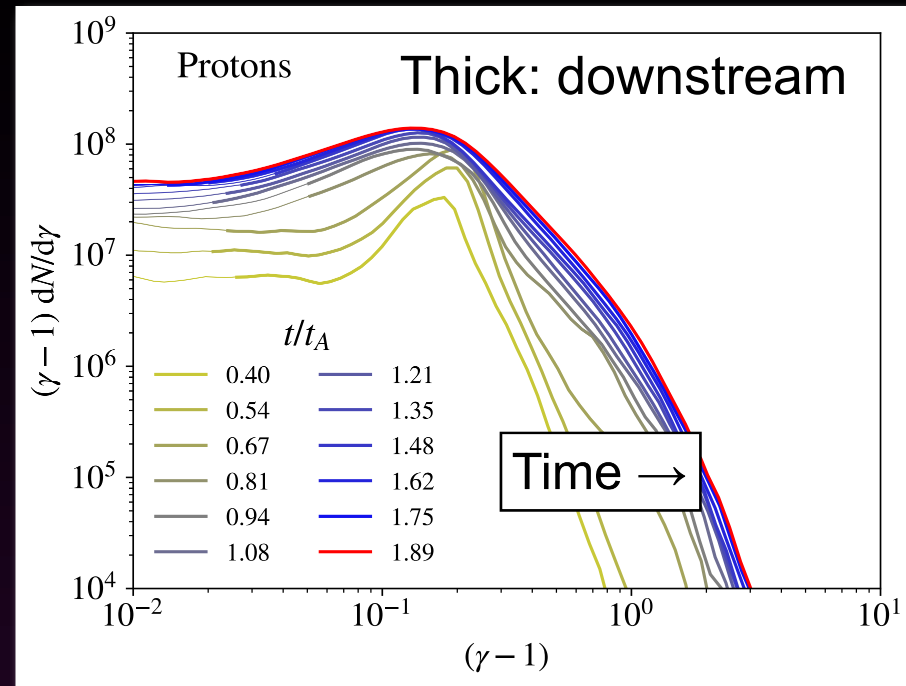

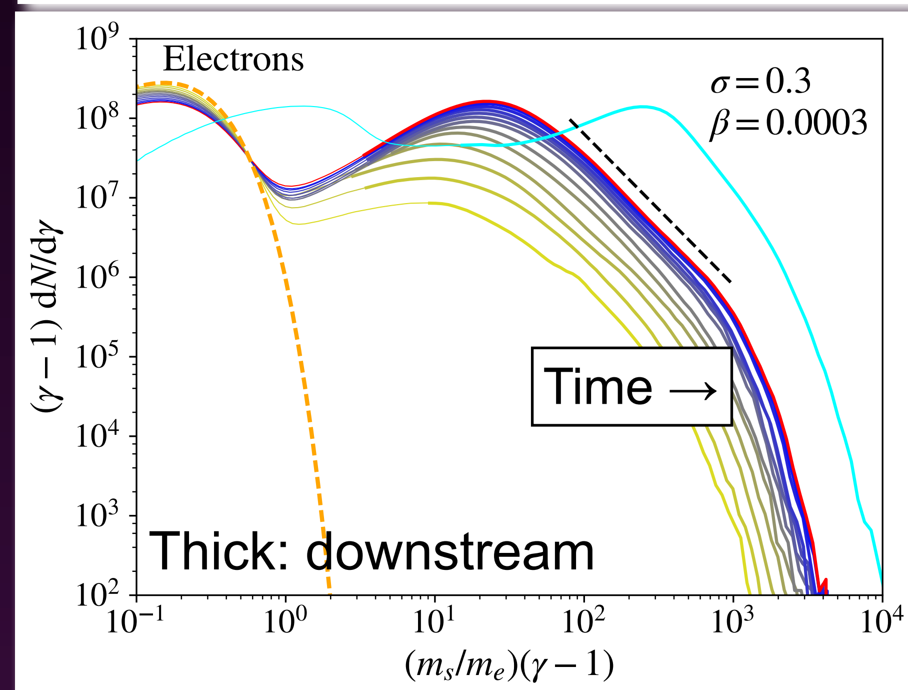

Protons: non-thermal tail only after the formation of the boundary island.

Electrons: well developed power law tail since early times.

Dependence on beta

$$\beta = \frac{8\pi n_0 k_B T}{B_0^2}$$

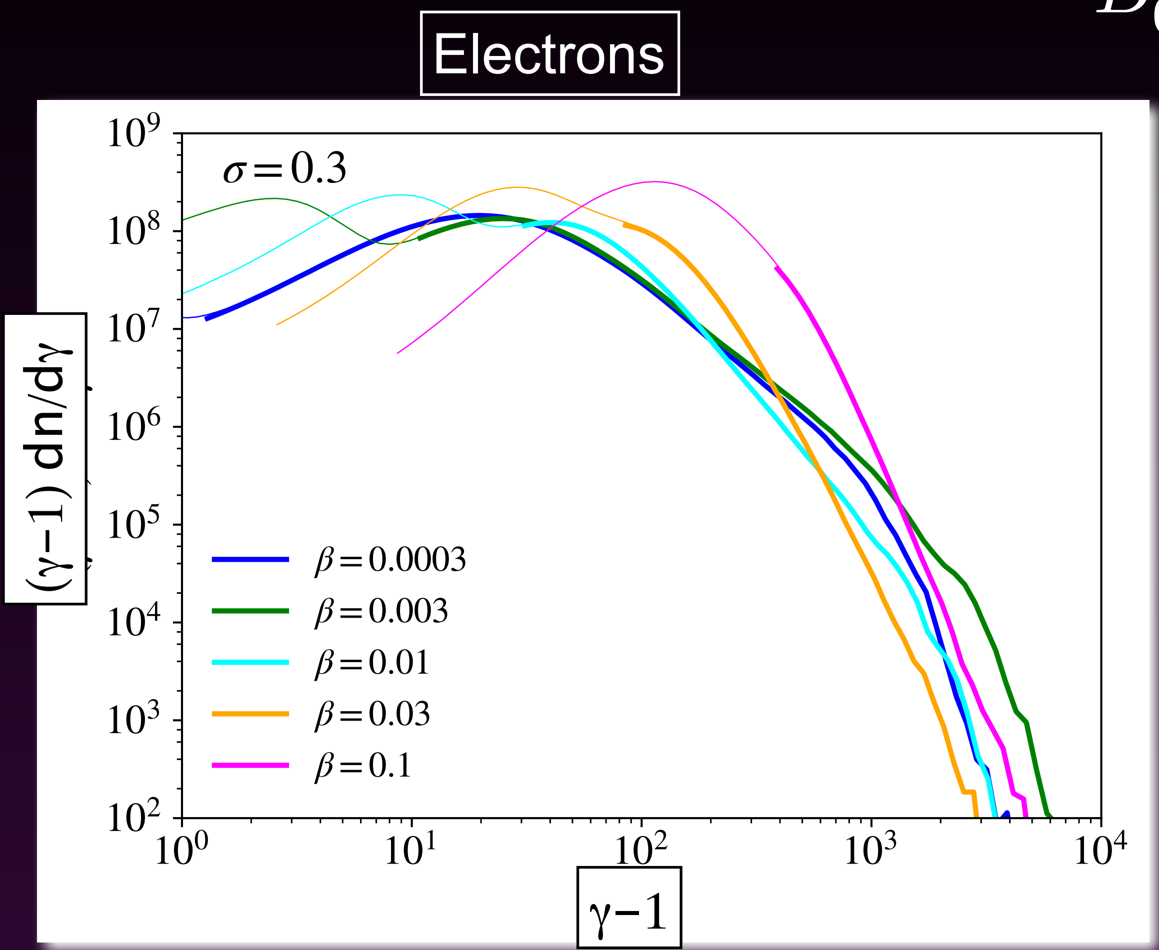

(Ball, LS & Ozel 2018)

- Lower beta:

- fragmentation into secondary plasmoids.

- hard electron spectra.

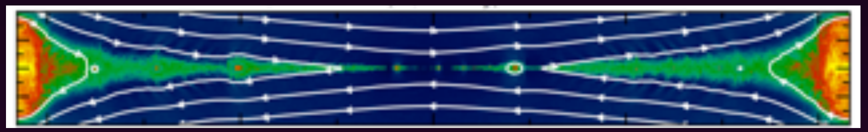

- Higher beta:

- smooth layer.

- steep electron spectra (nearly Maxwellian).

Dependence on beta and sigma

Electrons

$dn/d\gamma \propto \gamma^{-p}$

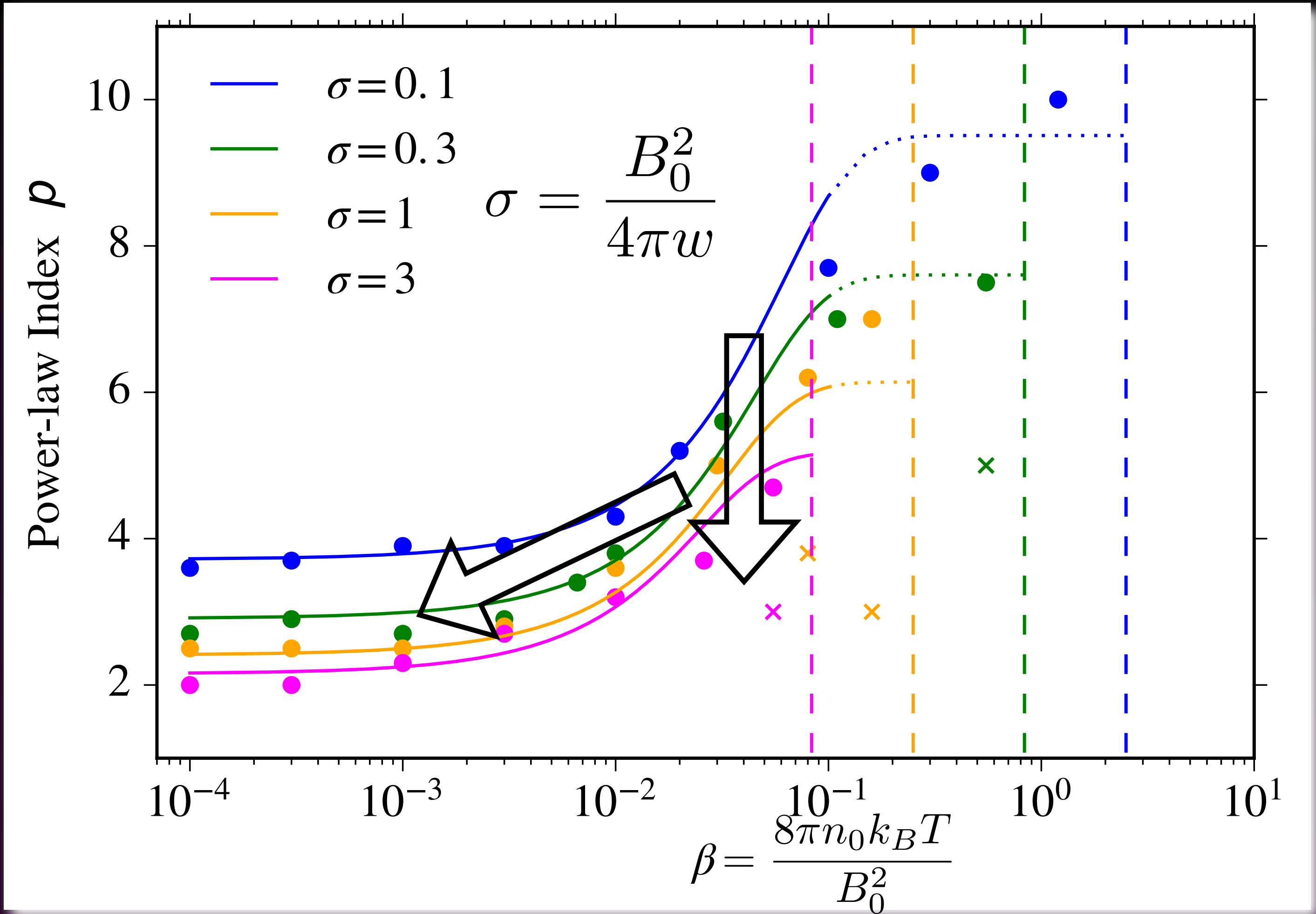

(Ball, LS & Ozel 2018)

- Harder slope for higher sigma (at fixed beta); see also Werner+18.
- Harder slope for lower beta (at fixed sigma).

Electron acceleration mechanism

σ=0.3 β=0.0003

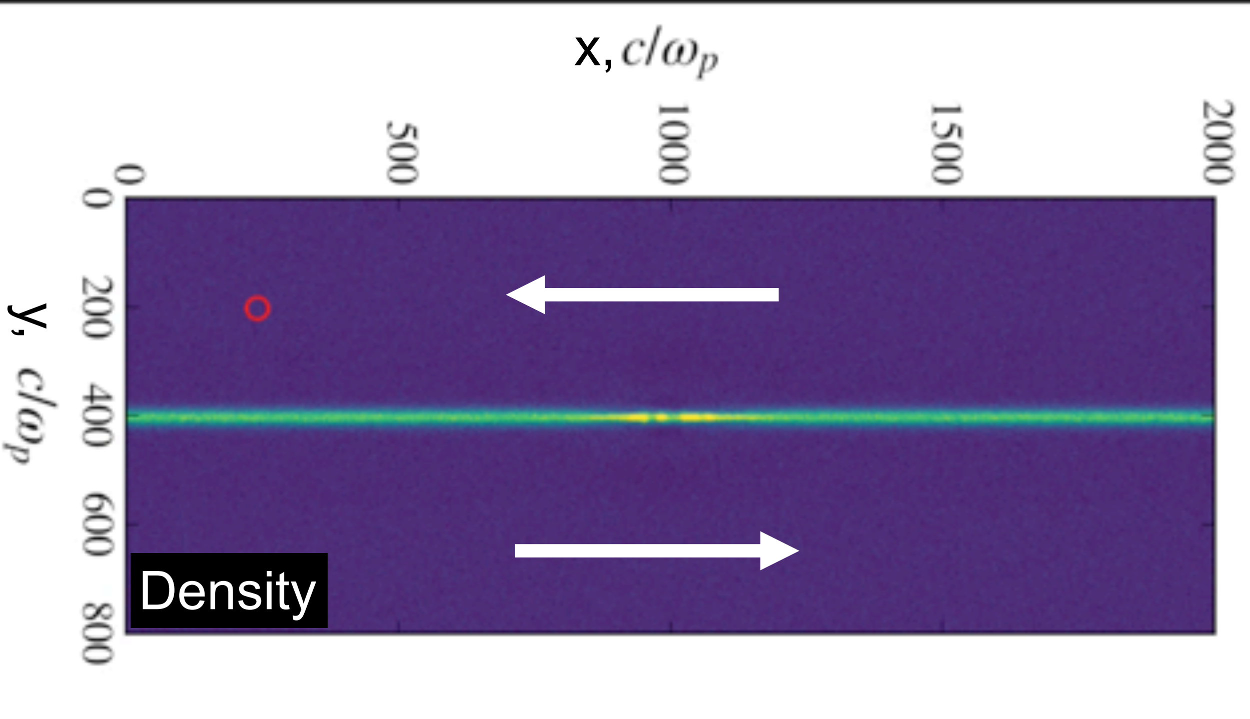

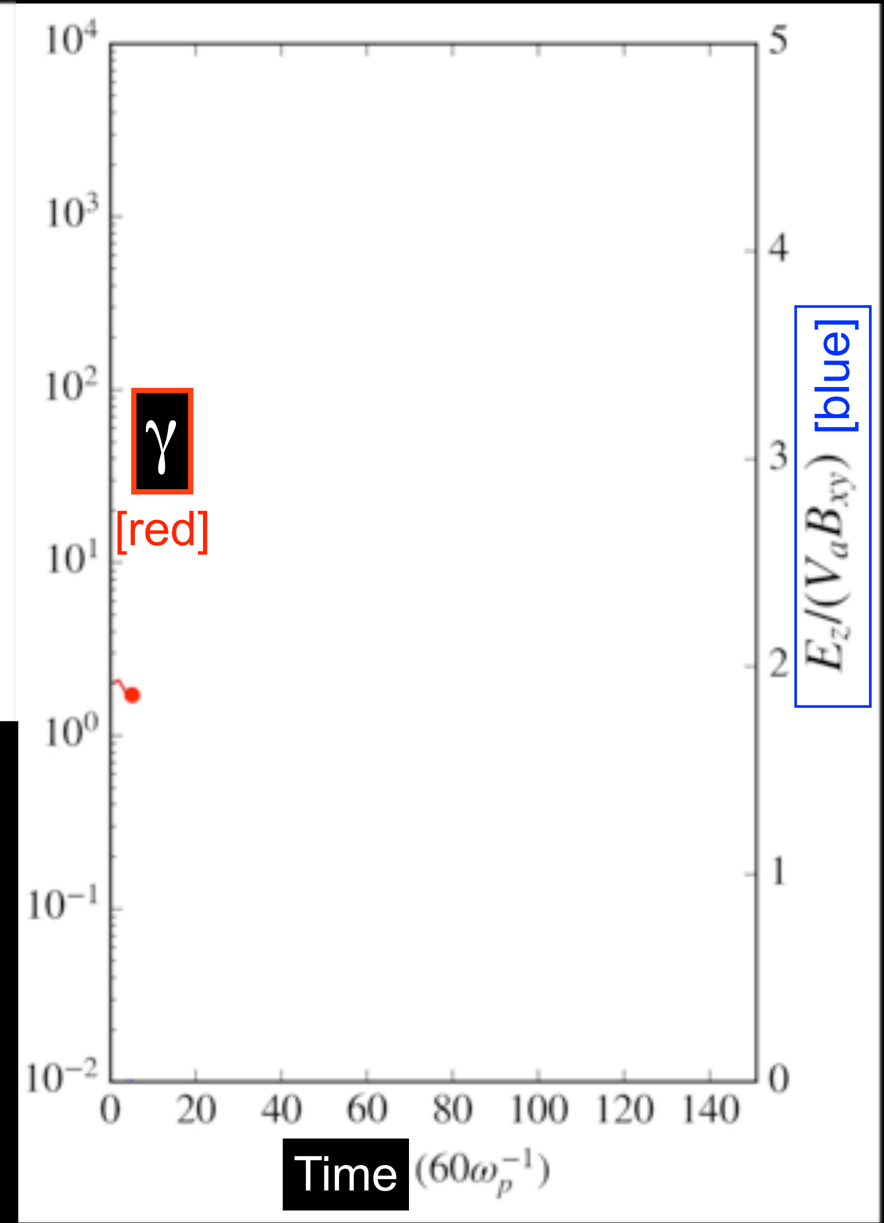

Two acceleration phases:

(a) at the X-point;

(b) in between merging islands

(Ball, LS & Ozel 2018)

Electron injection in reconnection

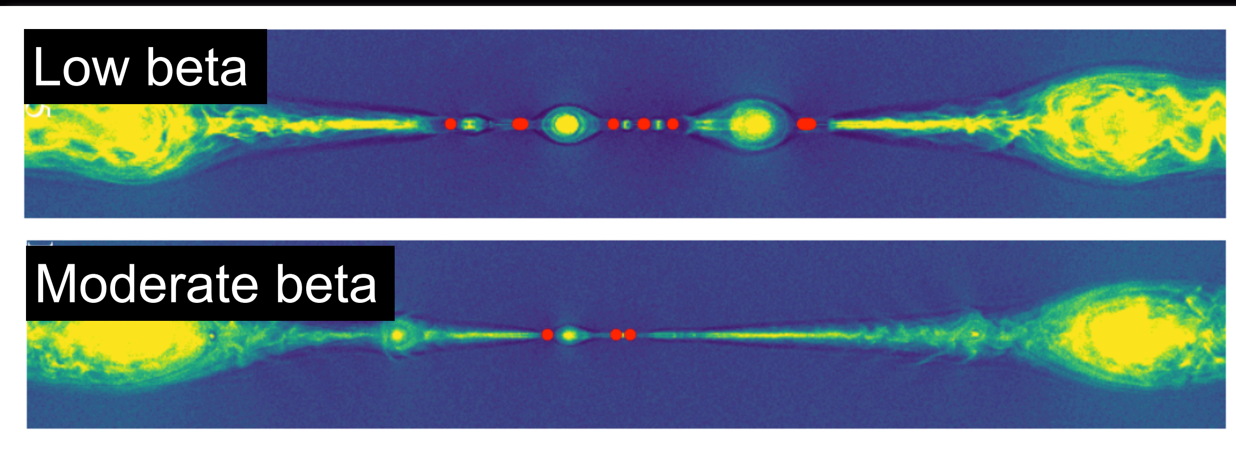

• Many more X-points (E>B) in low beta than in high beta.

X-point statistics

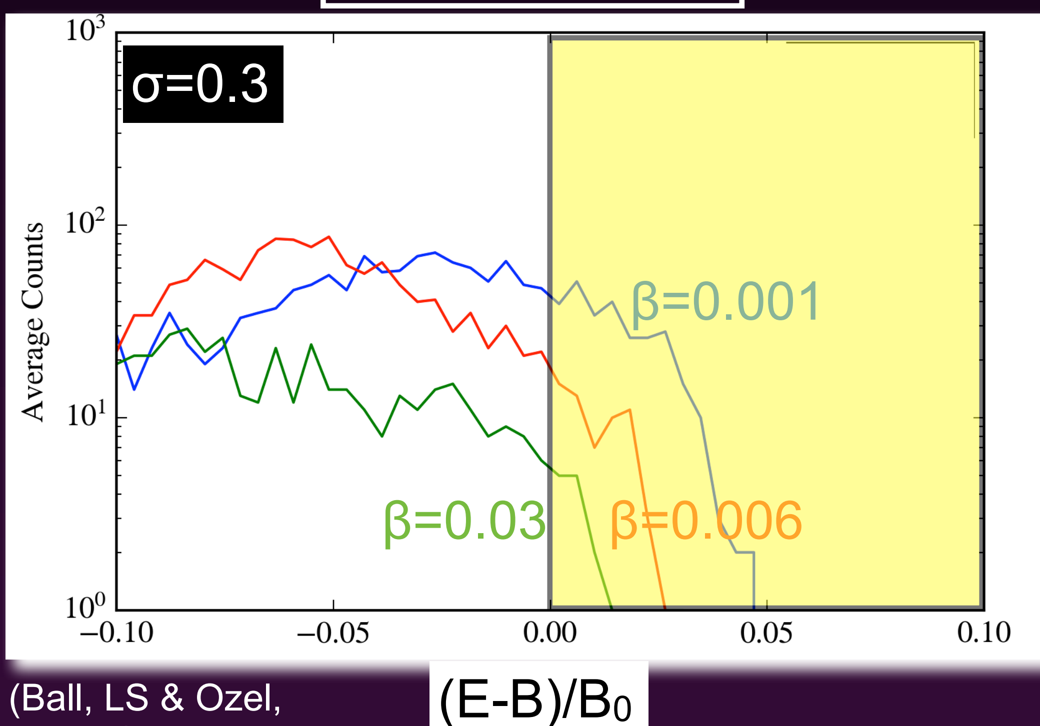

(Ball, LS & Ozel, in prep)

1. Electron injection at X-points (E>B).

2. More X-points for lower beta.

3. Acceleration is more efficient / harder slopes at lower beta.

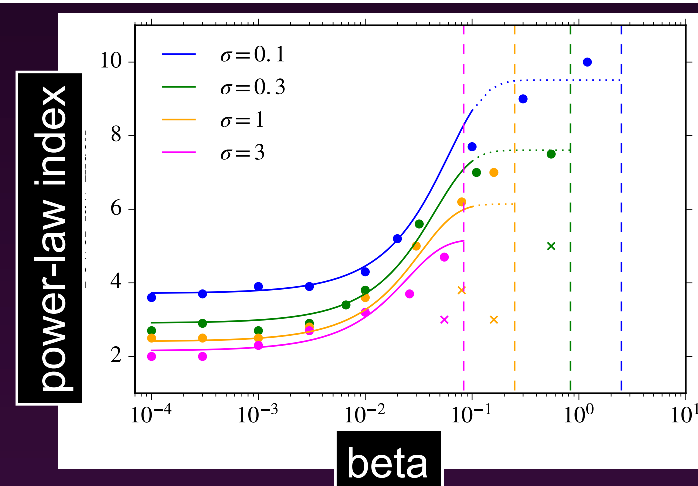

The special case of $\beta \sim \beta_{max} = 1/(4\sigma)$

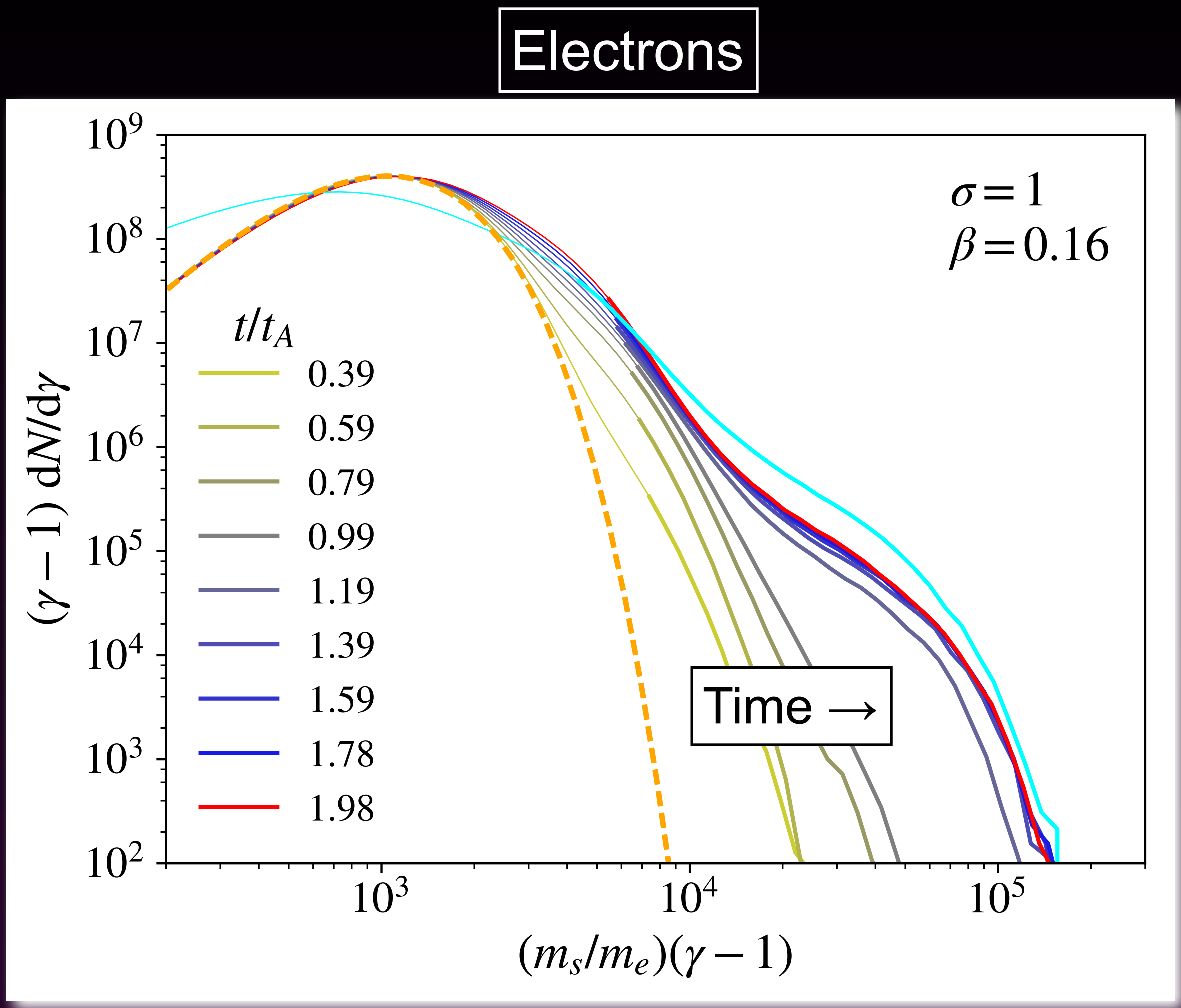

(Ball, LS & Ozel 2018)

For high beta, yet below $\beta_{max} \sim 1/(4\sigma)$, the electron spectrum is quasi-Maxwellian.

A power law emerges in the electron and proton spectra at $\beta_{max} \sim 1/(4\sigma)$, when both species start relativistically hot.

The special case of $\beta \sim \beta_{max} = 1/(4\sigma)$

$\sigma=1$ $\beta=0.16$

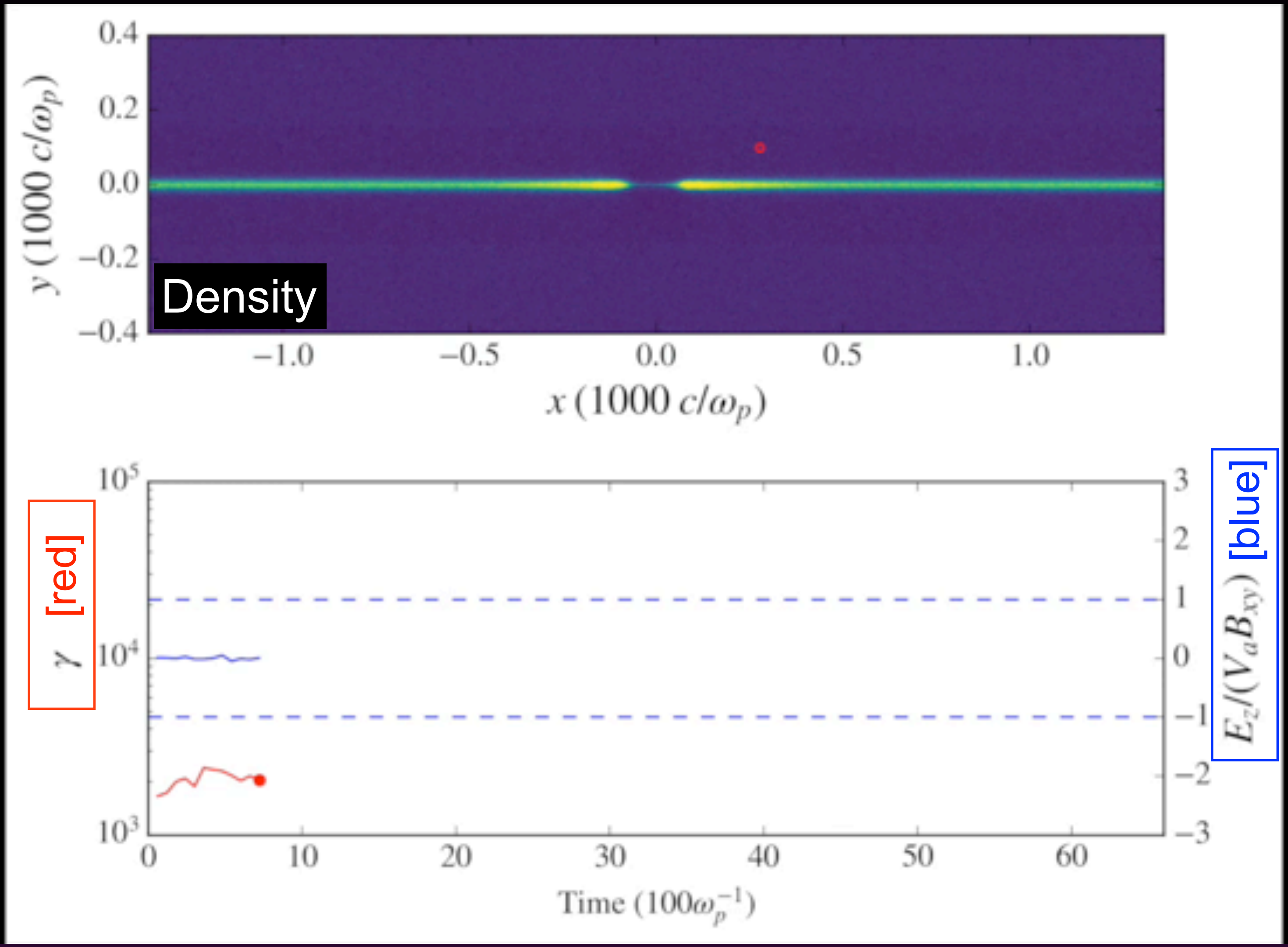

First kick in energy at the moment of interaction with the smooth outflow.

Second kick in a Fermi-like process between the outflow and the boundary island.

2. Reconnection in strong radiation fields

Accreting X-ray binaries

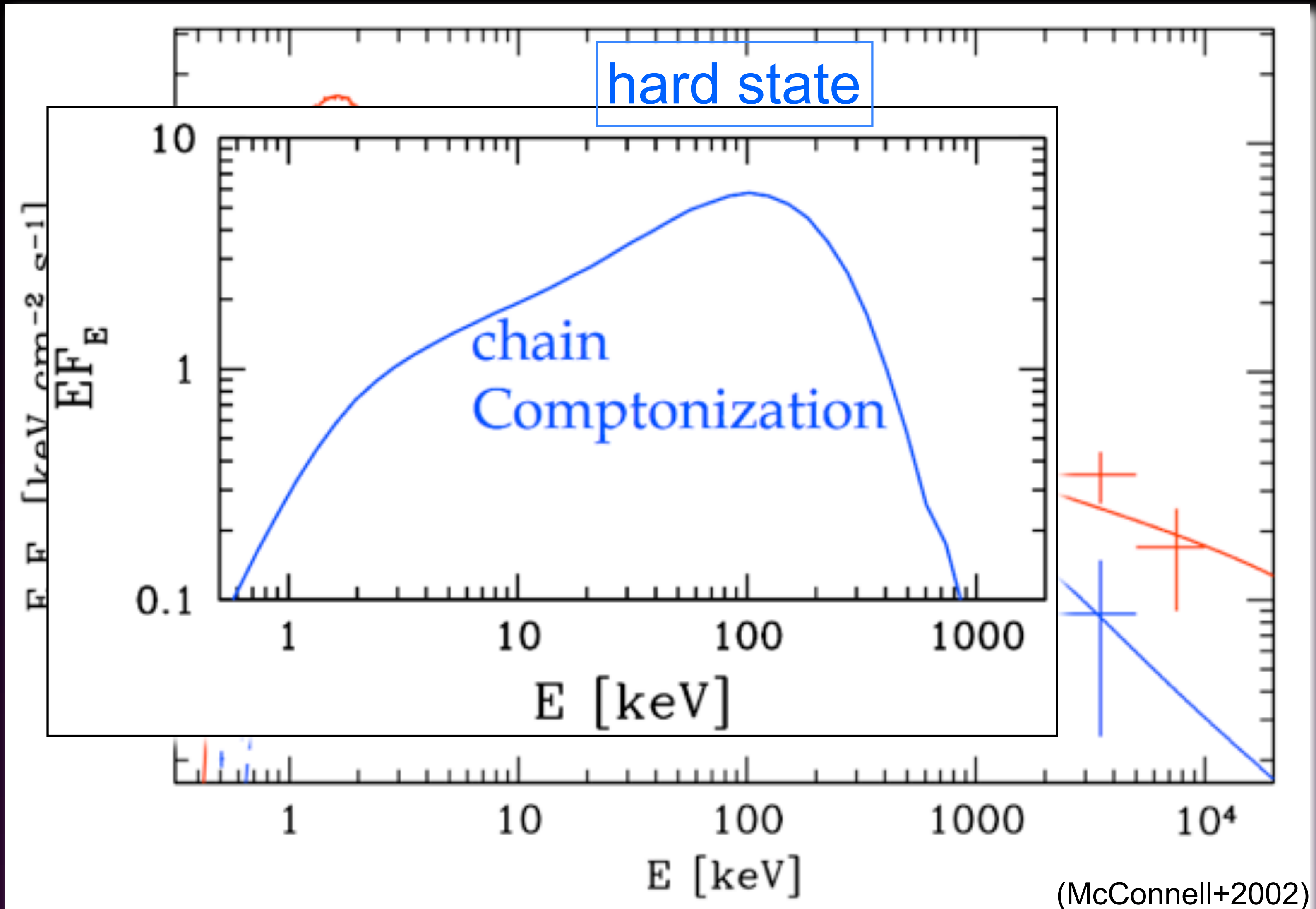

(McConnell+2002)

- Canonical interpretation: thermal Comptonization by hot plasma in a “corona” with electron temperature of ~100 keV.
- Alternative (Beloborodov 2017): bulk Comptonization by a radiatively-cooled plasmoid chain.

The plasmoid chain

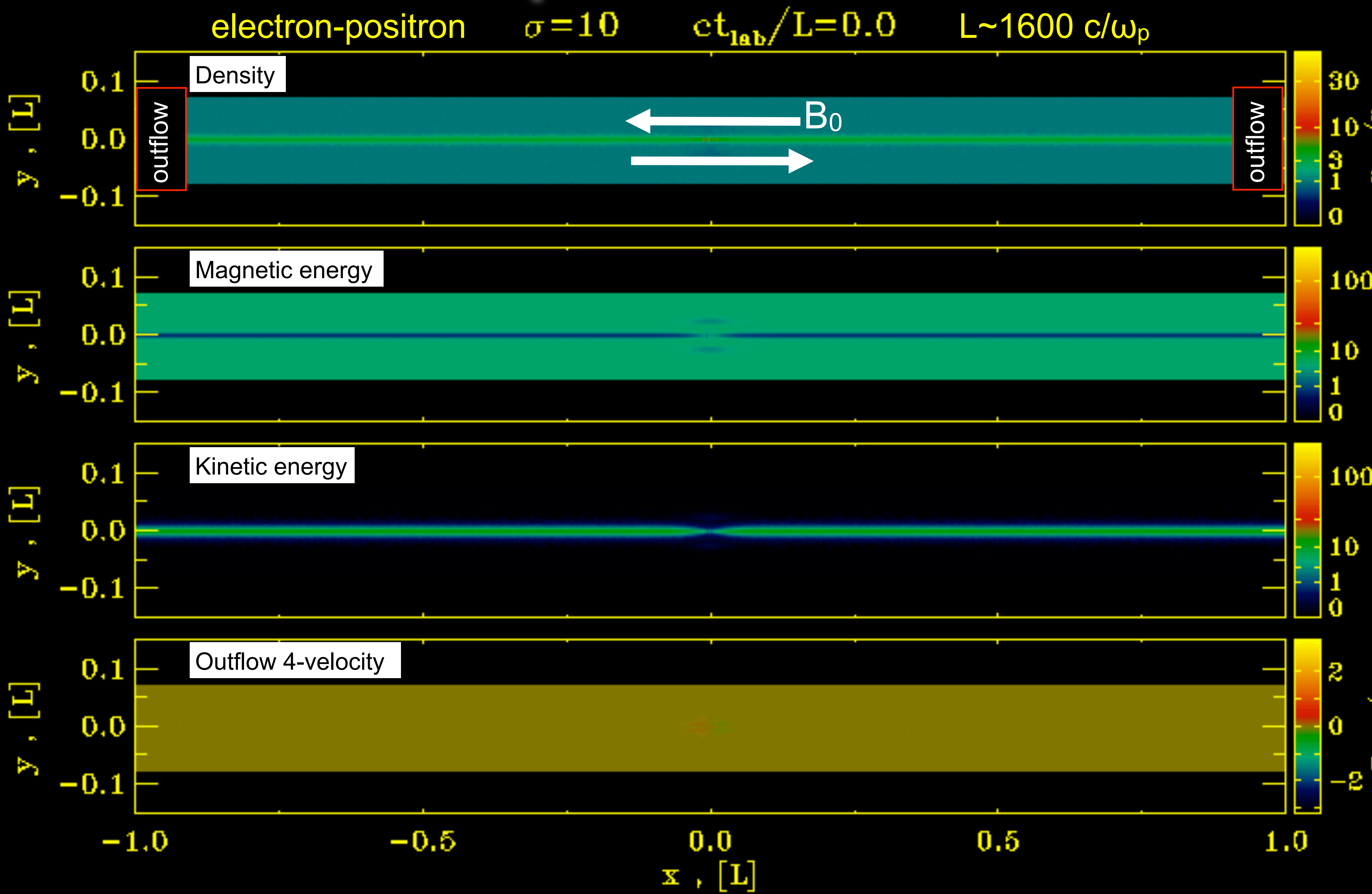

[see Maria Petropoulou's talk]

(LS, Giannios & Petropoulou 16)

Plasmoid space-time tracks

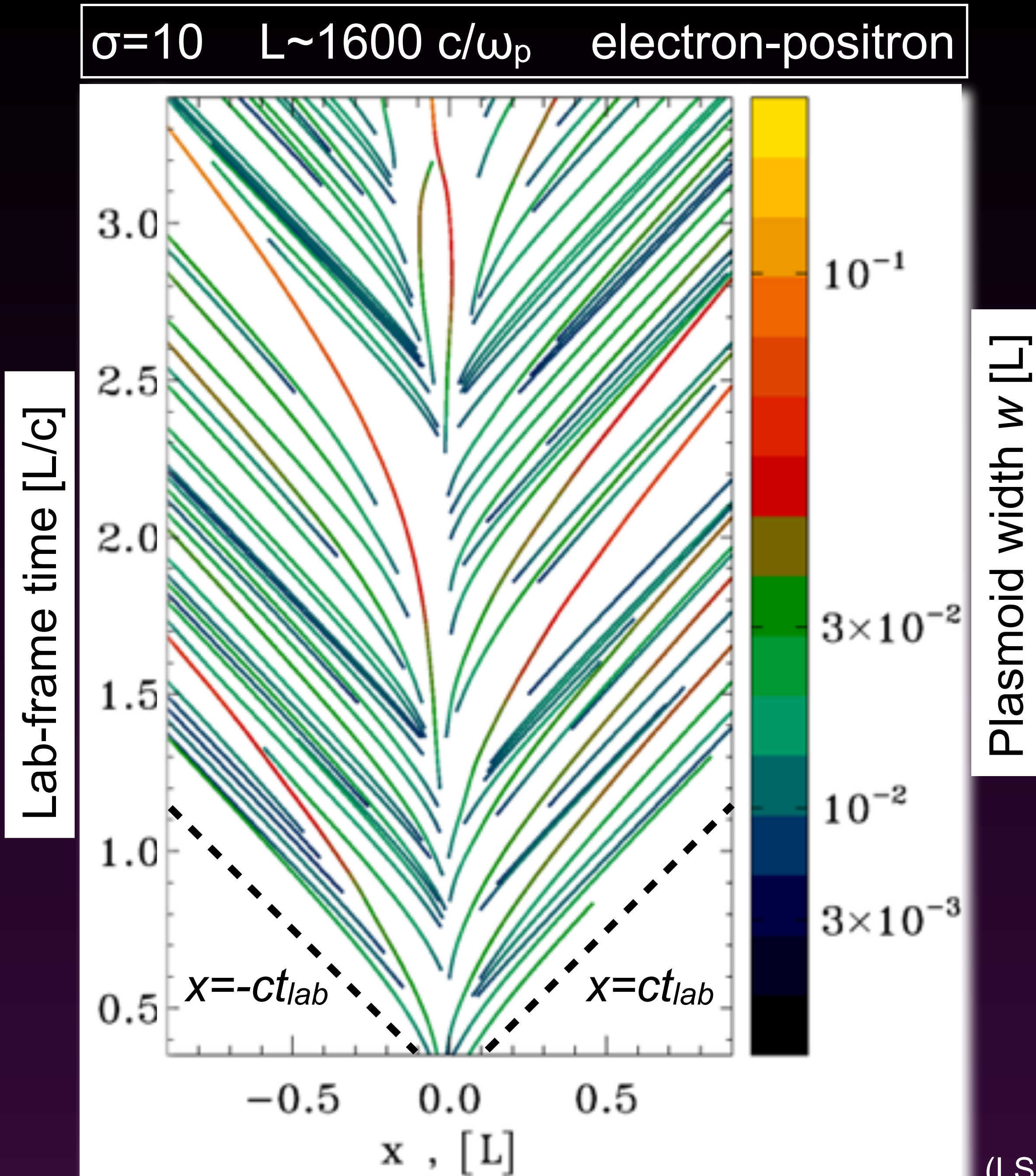

We can follow individual plasmoids in space and time.

First they grow, then they go:

- First, they grow in the center (at a rate ~0.1 *c*) while moving at non-relativistic speeds.
- Then, they accelerate outwards approaching the Alfven speed ~ *c*.

(LS, Giannios & Petropoulou 16)

Inverse Compton losses

The particles scatter off a prescribed isotropic photon field in the Thomson regime:

$$P_{IC} = \frac{4}{3}\sigma_T c \gamma^2 U_\star$$

In the ultra-relativistic limit, the Compton drag force is

$$\vec{f} = -P_{IC}\frac{\vec{v}}{c^2}$$

We parameterize the radiation energy density via a critical Lorentz factor γ_{cr} (balancing acceleration with IC losses):

$$eEc \sim \frac{4}{3}\sigma_T c \gamma_{cr}^2 U_\star \qquad E \sim 0.1B$$

What is the effect on particle acceleration and plasmoid dynamics?

Fix σ=10 and composition (electron-positron), vary γ_{cr}.

Weak IC losses

No cooling

$\gamma_{cr}=128=12.8\sigma$

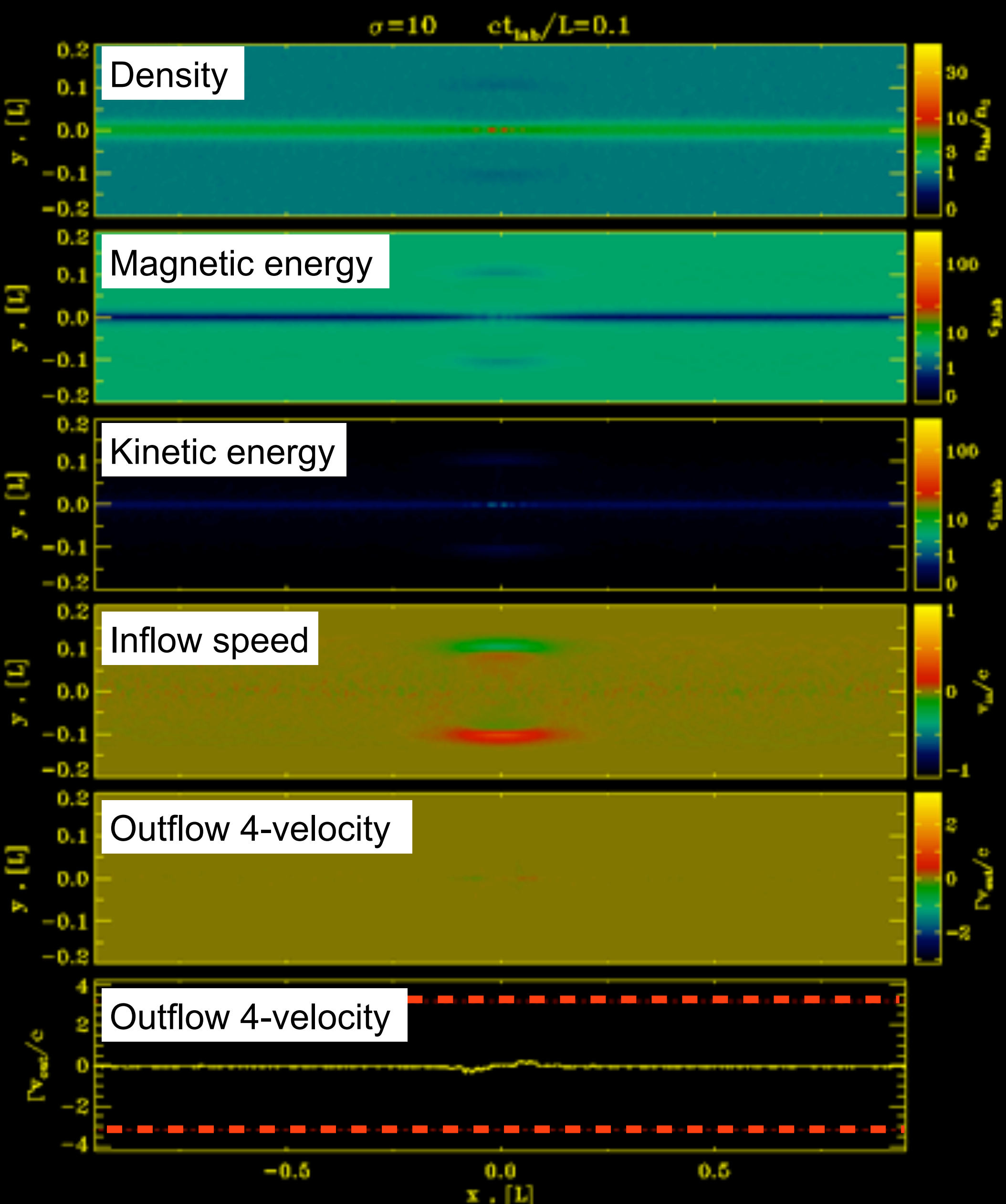

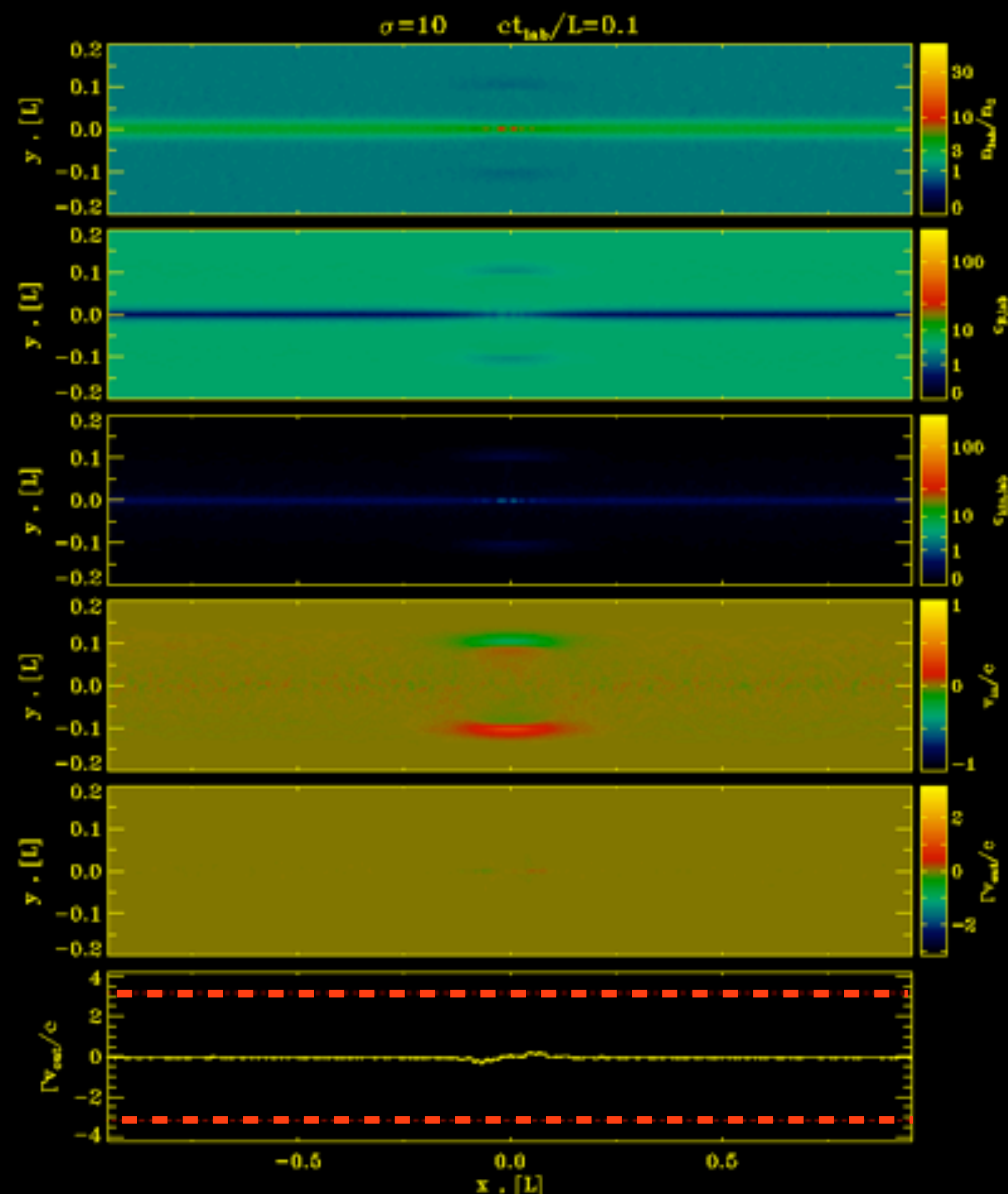

Weak IC losses

No difference in the inflow speed, outflow 4-velocity or plasmoid energy content.

The high-energy cutoff of the particle spectrum recedes to lower energies, due to IC cooling (see Werner's talk).

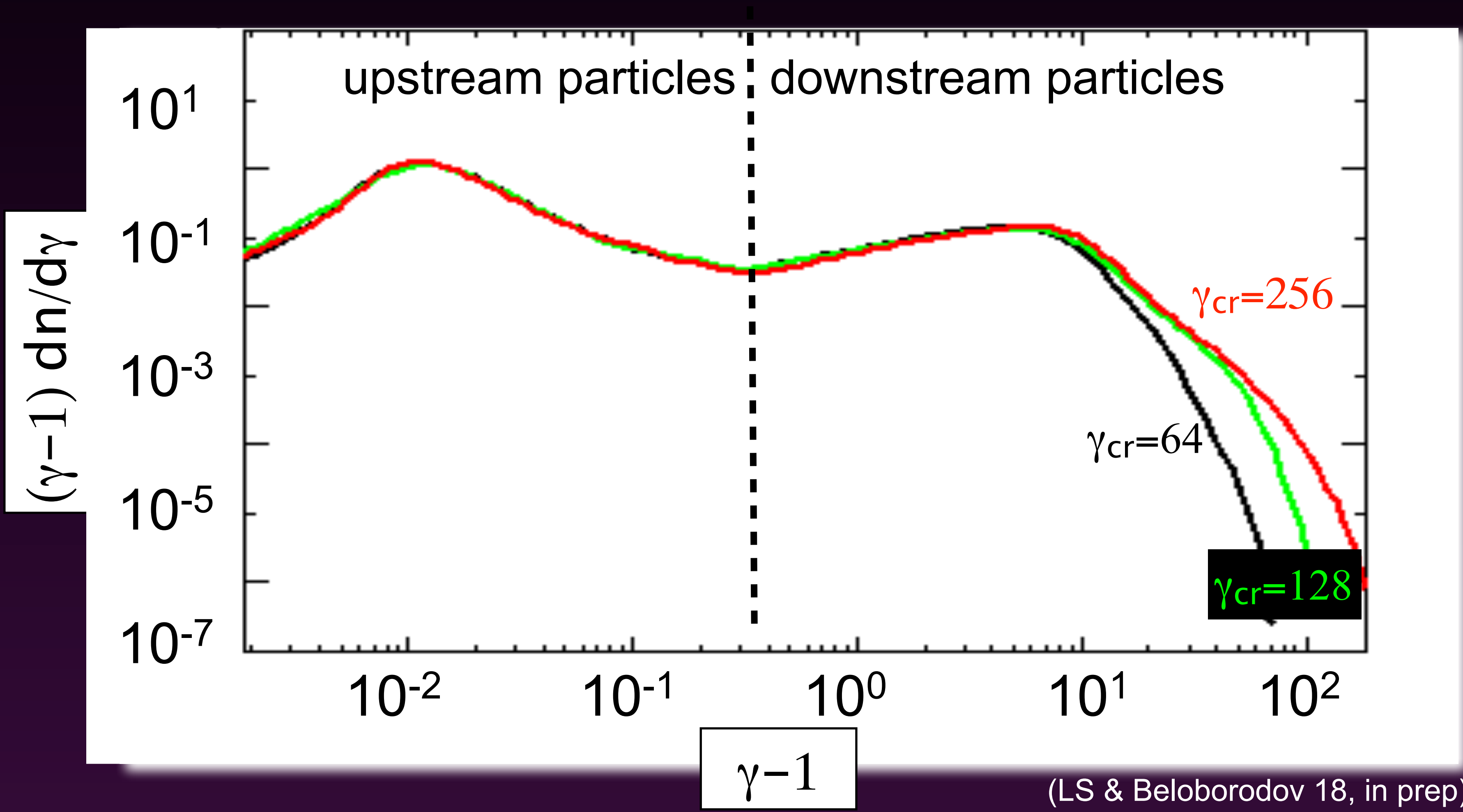

(LS & Beloborodov 18, in prep)

Moderate IC losses

No cooling

$\gamma_{cr}=16=1.6\sigma$

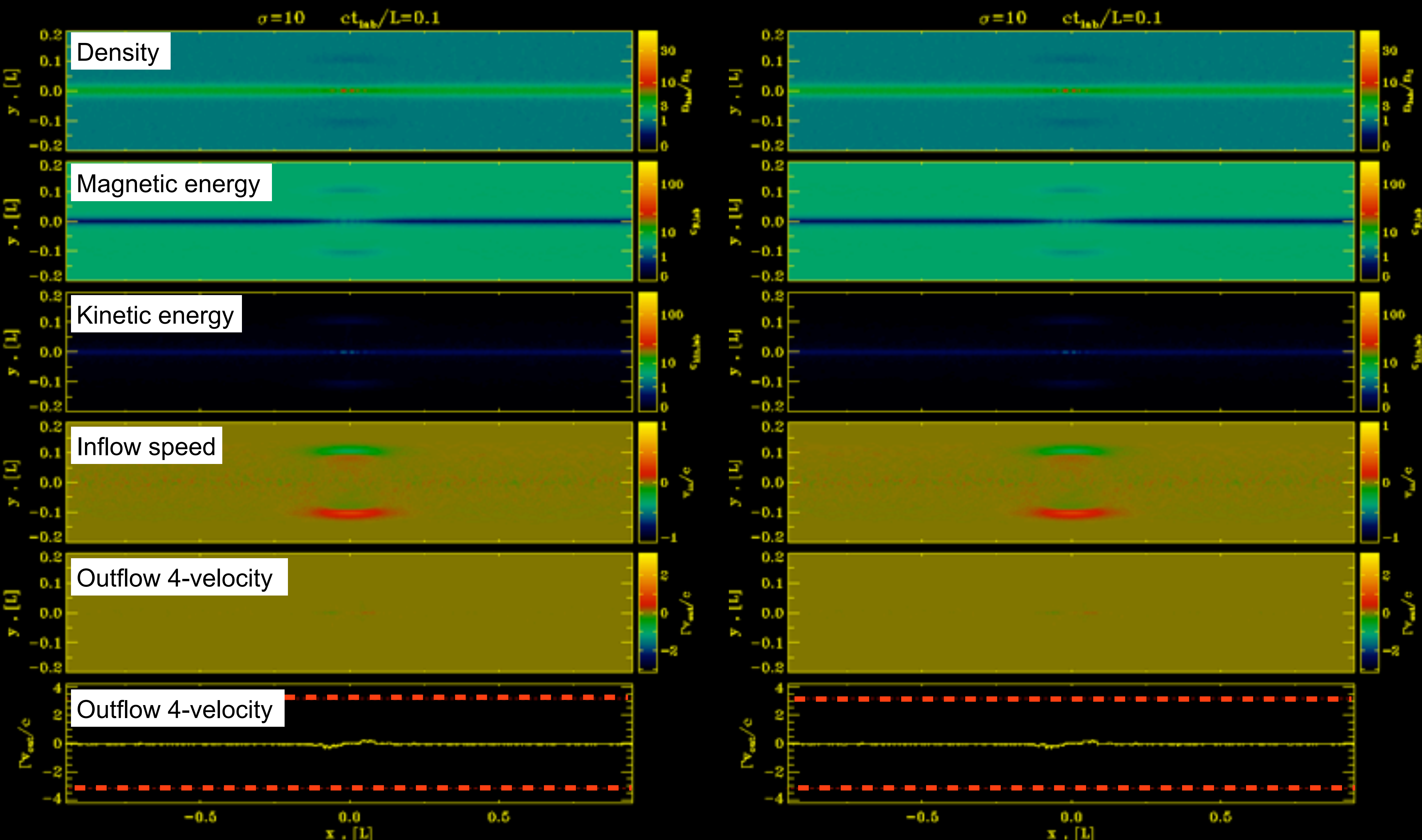

Moderate IC losses

No difference in the inflow speed and maximum outflow 4-velocity.

Effect of Compton drag depends on plasmoid size:

$$f_{push} = \xi \frac{U_B}{w} \qquad f_{drag} = \beta \Gamma^2 U_{\rm rad} \sigma_T n_\pm$$

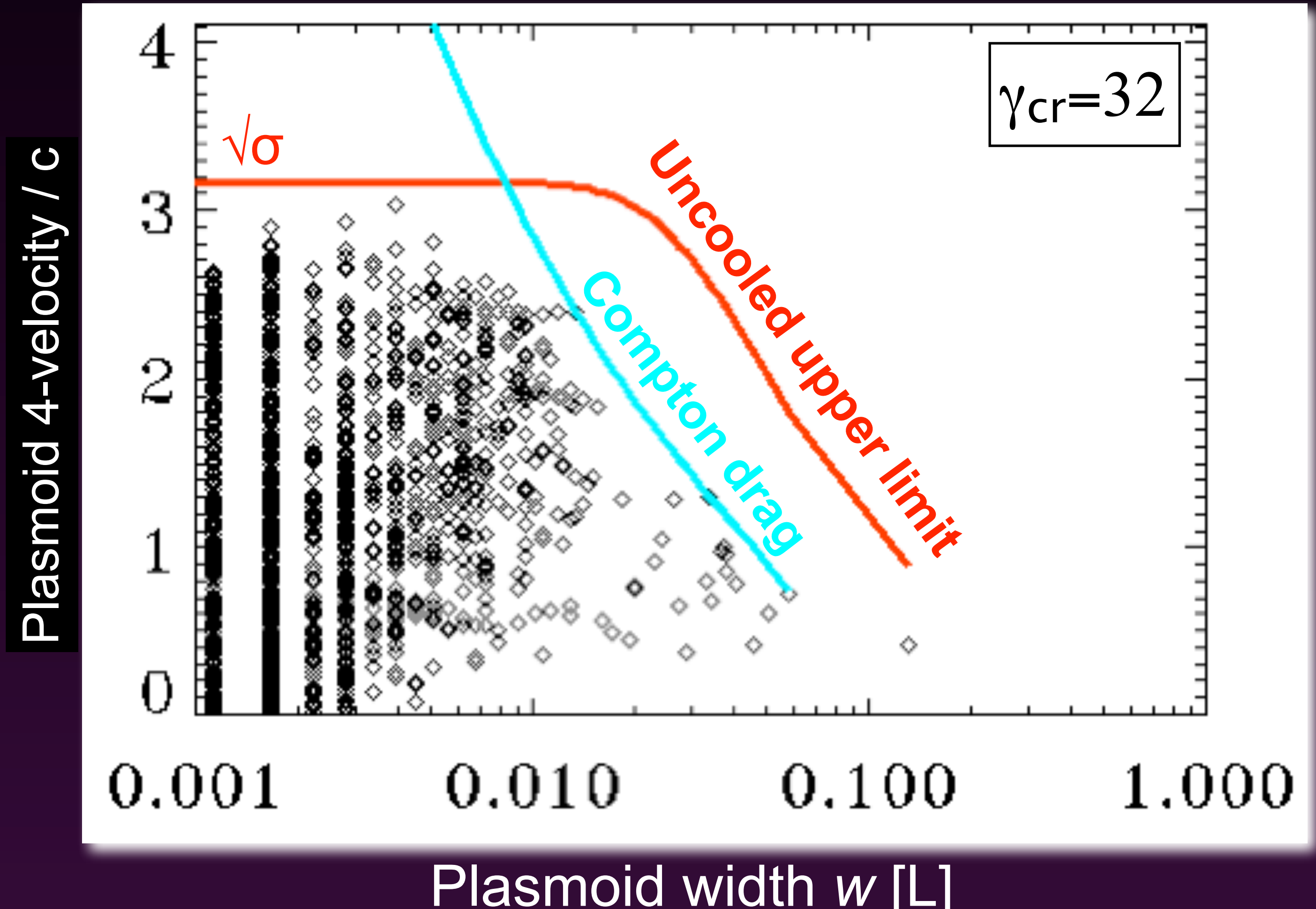

→ small plasmoids are unaffected, intermediate plasmoids are decelerated).

(LS & Beloborodov 18, in prep)

Strong IC losses

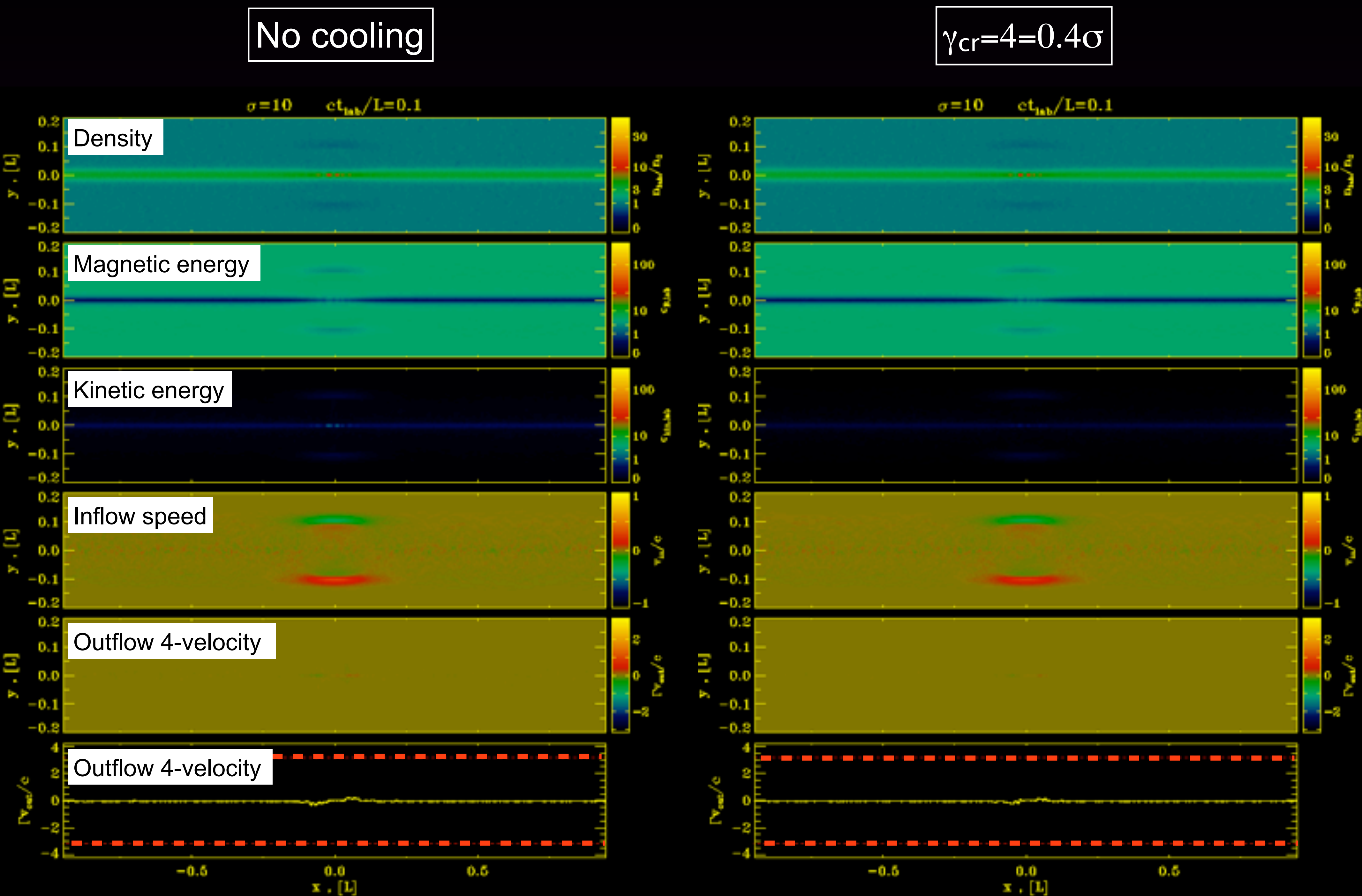

Strong IC losses

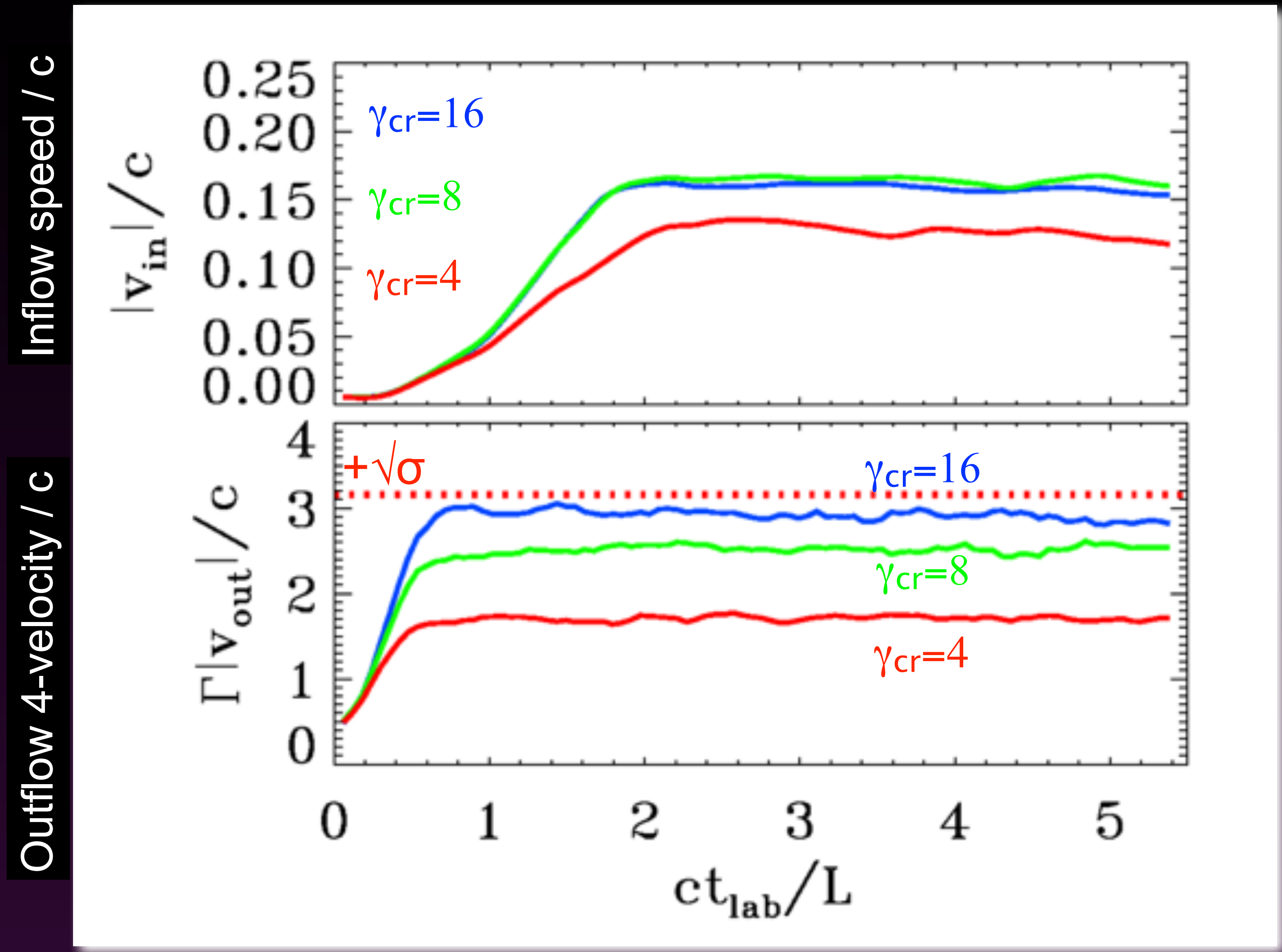

(LS & Beloborodov 18, in prep)

- No appreciable difference in the inflow speed (i.e., the reconnection rate).
- Strong suppression in the maximum outflow 4-velocity (Compton drag).

Summary

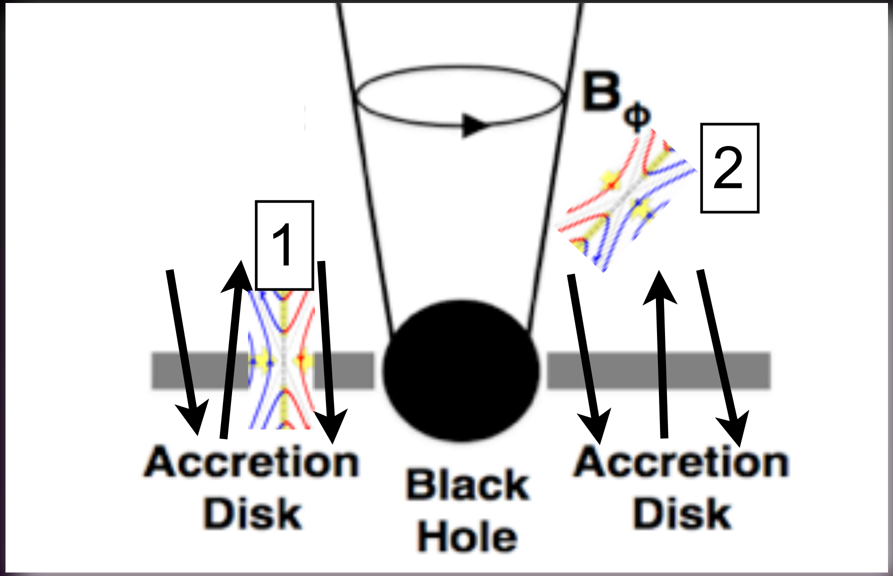

(1). Magnetized disks and coronae of collisionless accretion flows (like Sgr A* in our Galactic Center).

• Trans-relativistic reconnection (σ~1), electron-proton plasma.

- Electrons are heated less than protons (the heating ratio is ~0.2 at low sigma and beta).
- The power-law slope of accelerated electrons is harder for higher sigma and/or lower beta. Electrons are injected at X-points.

(2). Magnetized coronae in bright accreting binaries (Cyg X-1).

• Trans- and ultra-relativistic reconnection (σ~10) in strong radiation fields, pair-dominated.

- Compton drag can decelerate intermediate and large plasmoids, and in extreme cases slow down the whole outflow.
- Bulk Compton off the plasmoid chain can reproduce the hard state of accreting binaries.